1521-009X/49/11/972–984$35.00
DRUG METABOLISM AND DISPOSITION
https://doi.org/10.1124/dmd.121.000534
Drug Metab Dispos 49:972–984, November 2021

Identification of Food-Derived Isoflavone Sulfates as Inhibition Markers for Intestinal Breast Cancer Resistance Proteins[S]

Rina Agustina, Yusuke Masuo, Yasuto Kido, Kyosuke Shinoda, Takahiro Ishimoto, and Yukio Kato

Faculty of Pharmacy, Institute of Medical, Pharmaceutical and Health Sciences, Kanazawa University, Kanazawa, Japan (R.A., Y.M., K.S., T.I., Y.Ka.); Faculty of Pharmacy, Hasanuddin University, Makassar, Indonesia (R.A.); and Laboratory for Drug Discovery and Development, Shionogi & Co., Ltd., Toyonaka, Osaka, Japan (Y.Ki.)

Received for publication May 2, 2021. Accepted for publication Aug 16, 2021

ABSTRACT

Potential inhibition of the breast cancer resistance protein (BCRP), a drug efflux transporter, is a key issue during drug development, and the use of its physiologic substrates as biomarkers can be advantageous to assess inhibition. In this study, we aimed to identify BCRP substrates by an untargeted metabolomic approach. Mice were orally administered lapatinib to inhibit BCRP in vivo, and plasma samples were assessed by liquid chromatography/time of flight/mass spectrometry with all-ion fragmentation acquisition and quantified by liquid chromatography with tandem mass spectrometry. A differential metabolomic analysis was also performed for plasma from *Bcrp*$^{-/-}$ and wild-type mice. Plasma peaks of food-derived isoflavone metabolites, daidzein sulfate (DS), and genistein sulfate (GS) increased after lapatinib administration and in *Bcrp*$^{-/-}$ mice. Administration of lapatinib and another BCRP inhibitor febuxostat increased the area under the plasma concentration-time curve (AUC) of DS, GS, and equol sulfate (ES) by 3.6- and 1.8-, 5.6- and 4.1-, and 1.6- and 4.8-fold, respectively. BCRP inhibitors also increased the AUC and maximum plasma concentration of DS and ES after coadministration with each parent compound. After adding parent compounds to the apical side of induced pluripotent stem cell–derived small intestinal epithelial-like cells, DS, GS, and ES in the basal compartment significantly increased in the presence of lapatinib and febuxostat, suggesting the inhibition of intestinal BCRP. ATP-dependent uptake of DS and ES in BCRP-expressing membrane vesicles was reduced by both inhibitors, indicating inhibition of BCRP-mediated DS and ES transport. Thus, we propose the first evidence of surrogate markers for BCRP inhibition.

SIGNIFICANCE STATEMENT

This study performed untargeted metabolomics to identify substrates of BCRP/ABCG2 to assess changes in its transport activity in vivo by BCRP/ABCG2 inhibitors. Food-derived isoflavone sulfates were identified as useful markers for evaluating changes in BCRP-mediated transport in the small intestine by its inhibitors.

Introduction

The breast cancer resistance protein (BCRP) is a xenobiotic efflux transporter encoded by the *ABCG2* gene and is localized on the apical side of plasma membranes of cells of various organs (Vlaming et al., 2009). BCRP plays a vital role in drug absorption in the small intestine. Various BCRP substrate drugs have altered pharmacokinetics in subjects with ABCG2 gene polymorphisms (c.421C>A) as compared with wild-type subjects (Keskitalo et al., 2009; Mizuno et al., 2012; Gotanda et al., 2015). Among BCRP substrates, both sulfasalazine and rosuvastatin have been employed as in vivo probe drugs to assess BCRP inhibition mediated by other drugs (Lee et al., 2015); drug-drug interactions (DDIs), possibly via BCRP, have been suggested by the use of these drugs. For example, the AUC of rosuvastatin was reportedly increased after coadministration of febuxostat and osimertinib by 2.1- and 1.4-fold, respectively (Harvey et al., 2018; Lehtisalo et al., 2020), compared with rosuvastatin alone. In vitro inhibition studies have demonstrated potent inhibition of BCRP-mediated transport, with half-maximal inhibitory concentration (IC_{50}) values of ∼0.23 and 2 μM for febuxostat and osimertinib, respectively (Miyata et al., 2016; Harvey et al., 2018), indicating the clinical importance of BCRP inhibition by several types of compounds.

For safety assessment, the potential inhibition of BCRP is currently being evaluated during drug development. Endogenous substrates specific for each transporter are expected to be useful biomarkers to assess the in vivo inhibition potential of xenobiotic transporters to avoid the unnecessary administration of probe drugs to subjects. Clinical studies using endogenous substrates as biomarkers have been performed to evaluate the potential inhibition of various xenobiotic transporters. For example, coproporphyrin I and III have been proposed as endogenous substrates to assess the inhibition of organic anion–transporting polypeptide

This study was supported in part by a Grant-in-Aid for Scientific Research to Y.Ka. [Grant 18H02584] and Y.M. [Grant 18K06745] from the Ministry of Education, Culture, Sports, Science and Technology of Japan (MEXT) and Y.M. from the Japan Research Foundation for Clinical Pharmacology.

Yasuto Kido is an employee of Shionogi & Co., Ltd. (Osaka, Japan). This study was partially supported by a research fund from Shionogi & Co., Ltd.

dx.doi.org/10.1124/dmd.121.000534.

[S] This article has supplemental material available at dmd.aspetjournals.org.

ABBREVIATION: AIF, all-ion fragmentation; AUC, area under the plasma concentration-time curve; BCRP, breast cancer resistance protein; BS, biochanin A sulfate; DDI, drug-drug interaction; DS, daidzein sulfate; ES, equol sulfate; GS, genistein sulfate; iPS, induced pluripotent stem; LC-MS/MS, liquid chromatography with tandem mass spectrometry; LY, lucifer yellow; MS, mass spectrometry; MS/MS, tandem mass spectrometry; NMQ, *N*-methyl-quinidine; P-gp, P-glycoprotein; PLS-DA, projection to latent structures-discriminant analysis; SULT, sulfotransferase.

1B expressed in the liver, whereas taurine is transported into the kidney by organic anion transporter 1 (Lai et al., 2016; Tsuruya et al., 2016). Both *N*-methylnicotinamide and creatinine are endogenous substrates used to assess the inhibition of organic cation transporter 2 and multidrug and toxic compound extrusion 1/2K in the kidney (Chu et al., 2018). However, the application of such biomarkers has been limited to hepatic and renal uptake transporters. Biomarkers for xenobiotic efflux transporters, including BCRP, are yet to be comprehensively elucidated.

Numerous compounds have been identified as BCRP substrates among endogenous and food-derived compounds. These include uric acid, riboflavin, pheophorbide A, daidzein, and genistein. Among them, plasma concentrations of daidzein and genistein were reportedly increased in *Bcrp*$^{-/-}$ mice (Enokizono et al., 2007a). *Bcrp*$^{-/-}$ mice also exhibited an increase in phototoxicity caused by food-derived pheophorbide A (Jonker et al., 2002) along with the decreased secretion of riboflavin into the milk (van Herwaarden et al., 2007) and increased serum uric acid concentration (Ichida et al., 2012). Based on a comprehensive analysis using a metabolomic approach, systemic exposure to some phytoestrogen sulfates was found to be increased in *Bcrp*$^{-/-}$ mice (van de Wetering and Sapthu, 2012). Nevertheless, changes in these endogenous substrates after administering BCRP inhibitors have yet to be confirmed; therefore, their potential application as biomarkers to assess BCRP inhibition remains unclear.

Bcrp$^{-/-}$ mice are useful for revealing endogenous substrates when compared with wild-type mice; however, differences between the two strains do not necessarily indicate the effect of BCRP inhibitors. Accordingly, in the present study, we orally administered BCRP inhibitors to mice to identify BCRP substrates, including food-derived substrates, as possible biomarkers to assess BCRP inhibition. However, the disadvantage of this approach is the nonspecificity of inhibitors; therefore, *Bcrp*$^{-/-}$ mice were also employed for further screening. In this study, we first screened endogenous and food-derived BCRP substrates using an untargeted metabolomic approach. We evaluated BCRP inhibition by oral administration of the potent BCRP inhibitor lapatinib and assessed differences in plasma levels between *Bcrp*$^{-/-}$ and wild-type mice for identification of ion peaks of isoflavone sulfates commonly affected by the BCRP inhibitor and *Bcrp* gene knockout. The identified compounds were characterized by in vivo and in vitro studies using lapatinib and another BCRP inhibitor, febuxostat. In vivo characterization was performed in mice fed a diet composed of specific food-derived compounds. The effect of orally administered BCRP inhibitors was confirmed after oral coadministration of the parent compounds under normal dietary conditions. In vitro characterization was performed in induced pluripotent stem (iPS) cell-derived small intestinal epithelial-like cells to assess direct inhibition by small intestinal efflux transport inhibitors.

Materials and Methods

Materials. Lapatinib was purchased from LC Laboratories (Woburn, MA). Febuxostat was purchased from BLD Pharmatech (Shanghai, China). Daidzein, genistein, and equol 4′-sulfate were purchased from Cayman Chemical Company (Ann Arbor, MI). Equol was purchased from Tokyo Chemical Industry (Tokyo, Japan). Daidzein 4′-sulfate and genistein 7-sulfate were purchased from Toronto Research Chemicals (Toronto, ON, Canada). All other chemicals and reagents used were of analytical grade.

Animals. Male C57BL/6J mice (6–7 weeks old) were purchased from Japan SLC (Shizuoka, Japan). Mice were housed in standard environmental conditions and fed a chow diet (PicoLab Rodent Diet 20, Laboratory Supply, Fort Worth, TX) and tap water ad libitum. Mouse handling and experimental procedures were performed in accordance with the Kanazawa University guidelines for animal care and use. All protocols were approved by the Institutional Animal Care and Use Committee of Kanazawa University. *Bcrp*$^{-/-}$ mice with a C57BL/6J background were generated by disrupting the *Bcrp* gene by the zinc finger nuclease targeting of exon 4 of the gene, as previously described (Kido et al., submitted). All animal studies using *Bcrp*$^{-/-}$ and corresponding wild-type mice were approved by the Committee for Animal Care and Use at Shionogi & Co., Ltd.

Sample Preparation for Metabolomic Analysis. Six-week-old male C57BL/6J mice were fed 10% (w/w) roasted soybean flour (Shinsei Corporation, Aichi, Japan) for 2 weeks. One day prior to administering the BCRP inhibitor, mice were individually transferred to separate metabolic cages to prevent coprophagy during the experiment. Lapatinib (30 and 90 mg/kg) was suspended in a mixture of 1% (v/v) Tween 80 and 0.5% (w/v) hydroxypropyl methylcellulose and orally administered by gavage to the mice. Vehicle alone was administered as a control. After 1 hour, sulfasalazine suspended in 0.5% methylcellulose (5 mg/kg) was orally administered by gavage. Blood for untargeted metabolomic analysis was obtained from the inferior vena cava of anesthetized mice 7 hours after inhibitor or vehicle administration. Additionally, blood samples for untargeted metabolomics were obtained from *Bcrp*$^{-/-}$ and wild-type mice fed a normal chow diet. Plasma was immediately separated by centrifugation at 3,194 × g for 5 minutes and stored at −80°C until further analysis.

Metabolomic Analysis of Plasma Samples. Plasma samples were mixed with five volumes (v/v) of methanol containing diclofenac, which was used as an internal standard. This mixture was centrifuged (26,418 × *g*, 4°C, 10 minutes), and the supernatant was analyzed using the Acquity UPLC system coupled with Xevo G2 QTOFMS (Waters, Milford, MA). The measurement was performed using an Acquity bridged ethylene hybrid C18 column (2.1 × 100 mm, 1.7 μm, Waters). The mobile phases were solvent A, 5 mM ammonium acetate in water, and solvent B, 5 mM ammonium acetate in methanol. The gradient elution was performed as follows: 0–0.5 minutes, 95% A/5% B; 0.5–5.5 minutes, 95% A/5% B to 2% A/98% B; 5.5–7.5 minutes; 2% A/98% B; 7.5–7.6 minutes, 2% A/98% B to 95% A/5% B; 7.6–9.0 minutes, 95% A/5% B. The column temperature was maintained at 50°C, and the flow rate was 0.4 ml/min. The autosampler temperature was maintained at 4°C, and the injection volume was 3 μl. Data were obtained in the negative ion mode with a centroid format at *m/z* 100–600 on a quadrupole time-of-flight mass spectrometer, which was operated in all-ion fragmentation (AIF) mode, including four sequential acquisitions by alternating collision energies: full scan at 0 eV for 0.1 seconds, which was followed by tandem mass spectrometry (MS/MS) scans at 10, 20, and 40 eV for 0.1 seconds.

Data Processing and Multivariate Data Analysis. MS-DIAL software (version 4.38) (Tsugawa et al., 2019) was used to process the AIF-acquired data to detect and align peaks using the following parameters: minimum peak height for MS1, 1000; MS1 and MS2 tolerance, 0.01 Da; retention time tolerance for peak alignment, 0.3 minutes; MS1 tolerance for peak alignment, 0.1 Da; and more than two-thirds of samples were evaluated in each group. MS/MS spectra were obtained by retention time-based (Tsugawa et al., 2019) and correlation-based (Tada et al., 2020) deconvolution methods using the following parameters: minimum peak height for MS2 (1000) and minimum correlation coefficient (0.8). A multivariate data matrix containing information on sample identity, retention time, *m/z*, and peak intensities was generated. The data matrix was further analyzed using MetaboAnalyst (Chong et al., 2019) for projection to latent structures-discriminant analysis (PLS-DA) and volcano plots.

Effect of Oral Administration of BCRP Inhibitors on Plasma Concentration of Isoflavone Sulfates. Six-week-old male C57BL/6J mice were fed 10% (w/w) roasted soybean flour for 2 weeks, which was followed by transfer to separate metabolic cages on the day before BCRP inhibitor administration. Lapatinib (30 and 90 mg/kg), febuxostat (30 and 90 mg/kg), or vehicle alone was orally administered by gavage. Febuxostat was suspended in 0.5% (w/v) methylcellulose, and control experiments were performed using the corresponding vehicle for each compound. After 1 hour, sulfasalazine suspended in 0.5% methylcellulose (5 mg/kg) was orally administered by gavage. Blood samples were collected from the tail vein of nonanesthetized mice 1, 1.5, 2, 3, 5, and 7 hours after vehicle or inhibitor administration. The plasma samples were immediately separated and stored at −80°C until further analysis.

Disposition of Isoflavone Sulfates after Oral Administration of Their Parent Compounds with BCRP Inhibitors. Lapatinib (90 mg/kg) or vehicle alone was orally administered by gavage to 8-week-old male C57BL/6J mice fed a normal chow diet. After 1 hour, a mixture of daidzein and equol (3 and 10 mg/kg, respectively) suspended in 0.5% (w/v) methylcellulose was orally administered by gavage. Blood samples were collected from the tail vein of nonanesthetized mice

1, 1.25, 1.5, 2, 4, and 7 hours after inhibitor or vehicle administration. The plasma samples were immediately separated by centrifugation and stored at −80°C until further analysis.

Biliary and Urinary Excretion of Daidzein Sulfate after Oral Administration of Its Parent Compound. The bile ducts of 8-week-old male C57BL/6J mice fed a normal chow diet were cannulated with a polyethylene catheter (UT-03; Unique Medical, Tokyo, Japan) under isoflurane anesthesia. Lapatinib (90 mg/kg) or vehicle alone was orally administered by gavage. After 1 hour, daidzein (3 mg/kg) suspended in 0.5% (w/v) methylcellulose was orally administered by gavage. Bile samples were collected every 1 hour after oral administration of lapatinib or vehicle. For urine collection, 8-week-old male C57BL/6J mice fed a normal chow diet were transferred to separate metabolic cages the day before BCRP inhibitor administration. Lapatinib (90 mg/kg) or vehicle alone was administered by gavage. After 1 hour, daidzein (3 mg/kg) suspended in 0.5% (w/v) methylcellulose was orally administered by gavage. Urine samples were collected for 24 hours before lapatinib administration and every 24 hours after daidzein administration. The bile and urine samples were immediately stored at −80°C until further analysis.

Appearance of Isoflavone Sulfates in Human iPS Cell-Derived Small Intestine Epithelial Cells in the Presence of Their Parent Compounds and BCRP Inhibitors. Human iPS cell-derived small intestinal epithelial-like cells were obtained from Fujifilm (Tokyo, Japan) and cultured in cell culture inserts as previously described (Kabeya et al., 2020). After 23 days of culture, the culture medium was replaced with transport buffer (Hank's balanced salt solution buffer, pH 7.4) and preincubated at 37°C for 30 minutes. Then, additional preincubation was performed at 37°C for 30 minutes with or without lapatinib (0.1 μM and 1 μM) or febuxostat (10 μM) in both chambers. The medium volumes in the apical and basal chambers were 150 and 600 μl, respectively. Assays were initiated by replacing the buffer in the apical chamber with a mixture of daidzein, genistein, equol (1 μM each), and lucifer yellow (LY; 100 μM) with or without lapatinib or febuxostat. Aliquots (50 μl) of the buffer in the basal chamber were collected at 0, 15, 30, 60, and 120 minutes and replaced with an equal volume of the prewarmed fresh buffer. To determine LY in samples, fluorescence intensities were measured using a multimode plate reader (Spark10M, Tecan, Männedorf, Switzerland) at an excitation wavelength of 430 nm and an emission wavelength of 535 nm. To determine daidzein, genistein, equol, daidzein sulfate (DS), genistein sulfate (GS), and equol sulfate (ES), samples were mixed with five times methanol containing an internal standard (1 μM diclofenac). After centrifugation at 26,418 × *g* for 10 minutes at 4°C, supernatants were subjected to liquid chromatography with tandem mass spectrometry (LC-MS/MS).

Preparation of Membrane Vesicles. Expi293F cells cultured in suspension were transiently transfected with pcDNA3/BCRP and pcDNA3/P-glycoprotein (P-gp) using the ExpiFectamine 293 reagent (Thermo Fisher Scientific, Waltham, MA) according to the manufacturer's protocol. Seventy-two hours after transfection, cells were washed, suspended in 25 ml of hypotonic buffer (10 mM NaCl, 1.5 mM $MgCl_2$, 0.02 mM phenylmethanesulfonyl fluoride, and 10 mM Tris-HCl; pH 7.4), and placed on ice for 30 minutes. The cells were disrupted by nitrogen cavitation at 1,200 psi for 20 minutes at 4°C with gentle stirring in a pressure vessel (Parr, Moline, IL). The suspension was centrifuged at 4,000 × *g* for 10 minutes at 4°C, and the pellet was resuspended in 25 ml of hypotonic buffer to disrupt the cells by nitrogen cavitation. The lysate was centrifuged at 4,000 × *g* for 10 minutes at 4°C, and the supernatant was homogenized using a Dounce homogenizer (20 strokes). The homogenate was centrifuged at 1,000 × *g* for 10 minutes at 4°C. The supernatant was layered on top of a 35% sucrose solution (10 mM Tris-HCl, pH 7.4) and centrifuged in an SW 32 Ti rotor (Beckman Coulter, Brea, CA) at 18,000 × *g* for 90 minutes at 4°C. The white layer on the interface was collected using a 27G needle, diluted with 20 ml of suspension buffer (250 mM sucrose, 10 mM Tris-HCl, 0.02 mM phenylmethanesulfonyl fluoride; pH 7.4), and centrifuged at 100,000 × *g* for 120 minutes at 4°C. The pellet was suspended in the same buffer by passing through a 25G needle and further centrifuged at 100,000 × *g* for 180 minutes at 4°C. Finally, the pellet was resuspended in the same buffer, quickly frozen in liquid nitrogen, and stored at −80°C. Protein concentration was measured using a BCA protein assay (Thermo Fisher Scientific).

Transport Studies in Membrane Vesicles. Transport studies were performed using the membrane vesicles described above, as previously described (Omote and Moriyama, 2018). Briefly, 15 μl of reaction buffer (250 mM sucrose, 10 mM Tris-HCl, 10 mM $MgCl_2$, 10 mM creatinine phosphate, and 100 μg/ml creatinine kinase, pH 7.4, in the presence of 4 mM ATP or AMP) containing test compounds [3 μM of DS and ES, 10 μM LY, and 5 μM *N*-methyl-quinidine (NMQ)], were preincubated for 5 minutes at 37°C. To initiate transport, the reaction buffer was mixed with a vesicle suspension (5 μg protein) containing various concentrations of lapatinib, febuxostat, and KO143. After incubation for the designated times at 37°C, the reaction mixture was rapidly mixed with 50 μl of ice-cold stopping buffer (250 mM sucrose, 100 mM NaCl, and 10 mM Tris-HCl, pH 7.4) and centrifuged through a Sephadex G-50 Fine (Cytiva, Marlborough, MA) spin column at 760 × *g* for 2 minutes at 4°C to separate the vesicles from the medium. Fluorescence intensities of LY in the eluate were measured using a multimode plate reader as described above. To measure DS, ES, and NMQ, the eluate was mixed with five times methanol (v/v) containing an internal standard (1 μM diclofenac). After centrifugation at 26,418 × *g* for 10 minutes at 37°C, the supernatants were subjected to LC-MS/MS.

Sulfate Conjugation of Isoflavones in Cytosolic Fractions Prepared from the Mouse Small Intestines. Cytosolic fractions were prepared from small intestines of five 8-week-old male C57BL/6J mice as previously described (Kobayashi et al., 2012). Sulfate conjugation of isoflavones was determined as previously described (van de Wetering and Sapthu, 2012) with minor modifications. Briefly, 150 μl of reaction buffer (100 mM Tris-HCl, 5 mM $MgSO_4$, 2 μM dithiothreitol, pH 7.4) containing each compound (20 μM of daidzein, genistein, and equol) and cytosol (1 mg protein/ml) in the presence or absence of 5 mM ATP was incubated for 60 minutes at 37°C. The reaction was terminated by adding five times (v/v) ice-cold methanol containing internal standard. After centrifugation at 26,418 × *g* for 10 minutes at 37°C, the supernatants were subjected to LC-MS/MS.

Quantification by LC-MS/MS. Plasma samples were mixed with 12.5 volumes (v/v) of methanol containing midazolam and diclofenac as internal standards. This mixture was centrifuged at 26,418 × *g* for 10 minutes at 4°C, and the supernatant was subjected to LCMS-8040 (Shimadzu) using a C18-MS-II packed column (3 μm, 2.0 mm i.d. × 50 mm, Nacalai Tesque, Kyoto, Japan). The mobile phases were (A) 5 mM ammonium acetate in H_2O and (B) 5 mM ammonium acetate in methanol. The flow rate was 0.4 ml/min, and gradient elution was performed as follows: 0–0.3 minutes, 90% A/10% B; 0.3–0.8 minutes, 90% A/10% B to 65% A/35% B; 1.4–3.3 minutes, 99% A/1% B to 35% A/65% B; 3.3–4.7 minutes, 35% A/65% B to 2% A/98% B; 4.7–4.8 minutes, 90% A/10% B. Lapatinib, NMQ, and midazolam were measured in electrospray ionization positive mode (lapatinib: 581.1 > 365.0, NMQ: 339.0 > 58.0, midazolam: 326.0 > 291.2), whereas other compounds were measured in electrospray ionization negative mode (diclofenac: 294.1 > 250.0, febuxostat: 315.1 > 271.1, sulfasalazine: 397.0 > 197.1, daidzein: 253.1 > 208.1, genistein: 269.1 > 133.1, equol: 241.2 > 121.0, DS: 331.1 > 253.0, GS: 349.0 > 269.1, ES: 321.2 > 241.1). Regioisomers of isoflavone sulfates, such as 7′- and 4′-sulfates of daidzein, genistein, and equol were not evaluated in the present study because these regioisomers were not commercially available. The lower limit of quantification and interexperiment variations of LC-MS/MS are shown in Supplemental Table 1.

Statistical Analysis. Statistical analysis was performed using Student's *t* test and one-way ANOVA followed by Dunnett's multiple comparison test. All statistical analyses were performed using GraphPad Prism 7 (GraphPad Software, San Diego, CA).

Results

Screening of BCRP Substrates in Plasma of Mice Orally Administered with Lapatinib and in *Bcrp*$^{-/-}$ Mice. In the present study, we attempted to identify BCRP substrates within the body that can be employed as probes for assessing changes in BCRP function induced by BCRP inhibitor drugs. We adopted two BCRP inhibitors according to previous reports (Miyata et al., 2016; Yasuda et al., 2018), but the dose of febuxostat was modified to 90 mg/kg. We also included lower dose of lapatinib and febuxostat (30 mg/kg) to observe dose dependence. Accordingly, untargeted metabolomics of plasma samples was first performed to identify ion peaks in plasma altered after oral administration of lapatinib, a BCRP inhibitor. A previous study

investigated BCRP substrates using wild-type and *Bcrp*$^{-/-}$ mice fed a high-soy diet, as BCRP transports phytoestrogens and their metabolites (van de Wetering and Sapthu, 2012). In the present study, mice were fed a diet containing 10% (w/w) roasted soybean flour for 2 weeks to increase the presence of phytoestrogens and metabolites in the body. According to our preliminary analysis, the amount of typical phytoestrogens daidzein and genistein in a diet containing 10% (w/w) roasted soybean flour was approximately 3-fold higher than that in normal chow (unpublished data). A total of 1272 peaks were detected in the plasma samples of all groups examined. Vehicle- and low- (30 mg/kg) and high- (90 mg/kg) dose lapatinib groups were separated in the PLS-DA score plots (Fig. 1A). By comparing the vehicle and lapatinib high-dose groups, 135 peaks showed significant differences ($P < 0.05$) with a high fold increase (fold change > 2) (Fig. 1E). The peaks for lapatinib and sulfasalazine were confirmed by comparing the chromatogram and MS spectrum with those of standard compounds. Furthermore, spectra had several peaks with corresponding M+2 peaks, as in the chloride isotope pattern (^{35}Cl: ^{37}Cl = 3:1). Lapatinib contains chloride in its chemical structure, and these peaks were estimated to be derived from lapatinib and its metabolites.

In the present study, full mass scans in the AIF mode and deconvolution analysis were performed to obtain MS/MS spectra of all ions to detect chemical identities. BCRP preferentially transports sulfate conjugates (Mao and Unadkat, 2015), and sulfate conjugates often produce a common neutral fragment, SO_3, after collision-induced dissociation (Lafaye et al., 2004). Therefore, to select peaks possibly derived from sulfate conjugates, peaks with neutral loss of 79.96 ± 0.01 Da were identified from deconvoluted MS/MS spectra. Thirty-five peaks were identified in the lapatinib high-dose group, and among them, nine peaks were found to exhibit significantly higher signal intensities than those in the vehicle group ($P < 0.05$, fold change > 2) (Fig. 1F), as shown in Table 1. These peaks were designated peaks #1 to #9 based on their retention times (Table 1). By comparing their retention time and fragmentation patterns with those of authentic compounds, peaks #2 and #5 were identified as DS and GS, respectively. A low dose of lapatinib (30 mg/kg) increased DS and GS by 2.9- and 2.8-fold, respectively, whereas a high dose of lapatinib (90 mg/kg) exhibited higher fold change (5.1- and 5.9-fold, respectively), showing a dose-dependent effect on BCRP inhibition. Peaks #7 and #8 were assumed to be debenzylated lapatinib (M1)-sulfate, which is reportedly formed after incubation of lapatinib with human S9 in the presence of 3′-phosphoadenosine 5′-phosphosulfate (Nardone-White et al., 2021). Peak #3 was assumed to be biochanin A sulfate, a substrate of BCRP (An and Morris, 2011), but the reference standard was not commercially available. Other peaks, including peaks #1, #4, #6, and #9, remained unidentified.

Untargeted metabolomic analysis of plasma samples obtained from *Bcrp*$^{-/-}$ and wild-type mice was also performed. A total of 962 peaks were detected in plasma samples from both strains, and *Bcrp*$^{-/-}$ and wild-type mice were clearly separated in the PLS-DA score plots (Fig. 1B). By comparing *Bcrp*$^{-/-}$ and wild-type mice in the volcano plot, 51 peaks exhibited significant differences ($P < 0.05$), with high fold increases (fold change > 2) (Fig. 1G). Ions with a neutral loss of 79.96 ± 0.01 Da were searched, and 27 peaks were selected in both strains (Fig. 1H). Among them, three ion peaks, DS, BS, and GS, showed higher signal intensity in both the lapatinib high-dose group (Table 1) and *Bcrp*$^{-/-}$ mice when compared with the vehicle group and wild-type mice, respectively. Other peaks remained unidentified (Fig. 1H).

Effect of BCRP Inhibitors on the Disposition of Isoflavone Sulfates Derived from Diets. Next, we attempted to confirm the effect of orally administered BCRP inhibitors on the disposition of two isoflavone sulfates (DS and GS) identified in the two untargeted metabolomic analyses as well as ES transported by BCRP in vitro (van de Wetering and Sapthu, 2012), which is commercially available. The plasma concentration of the typical BCRP substrate sulfasalazine was first examined and found to be increased after oral coadministration of lapatinib in mice fed a roasted soybean flour–containing diet, confirming BCRP inhibition by lapatinib (Fig. 2A). In the same mice, plasma concentration profiles of DS, GS, and ES were also found to be increased after oral administration of lapatinib (Fig. 2, B–D). Oral administration of lapatinib (30 and 90 mg/kg) increased the C_{max} and $AUC_{0\text{-}7h}$ values of sulfasalazine, DS, GS, and ES (Table 2). The AUC of DS, GS, and ES of the vehicle-, low-, and high-dose lapatinib-treated mice showed positive correlations with that of sulfasalazine (Supplemental Fig. 2A). Furthermore, lapatinib increased the C_{max} and $AUC_{0\text{-}7h}$ values of the parent compounds daidzein and genistein (Supplemental Table 2), which is consistent with a previous report showing that daidzein and genistein are substrates of BCRP (Enokizono et al., 2007a); however, these absolute values were much lower than those of their sulfates (Table 2). Although lapatinib concentrations in plasma after treatment with 90 mg/kg were higher than those of treatment with 30 mg/kg (Supplemental Fig. 3A), an apparent increase in $AUC_{0\text{-}7h}$ values of DS, GS, and ES was not clearly observed with increasing lapatinib concentrations (Table 2).

To further evaluate the effect of orally administered BCRP inhibitors on the disposition of DS, GS, and ES, another BCRP inhibitor, febuxostat (Miyata et al., 2016), was also administered to mice fed a diet containing roasted soybean flour. Similar to the findings after lapatinib administration, febuxostat significantly increased the plasma concentration of sulfasalazine after oral administration (Fig. 2E). The C_{max} and $AUC_{0\text{-}7h}$ values of sulfasalazine, DS, GS, ES, daidzein, and genistein were increased after oral administration of febuxostat (30 and 90 mg/kg); however, only the increased $AUC_{0\text{-}7h}$ value of GS was significant among the assessed isoflavones (Supplemental Table 2; Table 3). The AUC of DS, GS, and ES in the vehicle-, low- and high-dose febuxostat-treated mice tended to exhibit positive correlations with that of sulfasalazine (Supplemental Fig. 2B). Overall, these results suggest that food-derived isoflavone sulfates were increased after oral administration of the BCRP inhibitors lapatinib and febuxostat.

Effect of Oral Administration of BCRP Inhibitors on the Disposition of Isoflavone Sulfates after Oral Administration of Parent Compounds. Next, we evaluated the effect of BCRP inhibitors on the disposition of isoflavone sulfates. Accordingly, plasma concentration profiles of DS and ES after oral administration of parent isoflavones (daidzein and equol) were examined in mice fed a normal chow diet with or without lapatinib coadministration. Lapatinib significantly increased plasma concentrations of DS and daidzein (Fig. 3, A and C), and the $AUC_{1\text{-}7h}$ values of these compounds increased after oral administration of daidzein at 3 and 10 mg/kg (Table 4). At these doses, differences in C_{max} and $AUC_{1\text{-}7h}$ of daidzein and DS were not substantially apparent when the daidzein dose differed 3-fold, indicating the nonlinear disposition of these compounds (Table 4). Nonlinear pharmacokinetics have been reported for GS after genistein administration (Yang et al., 2012), but no report has clarified the pharmacokinetics of DS or ES. Nevertheless, the $AUC_{1\text{-}7h}$ ratio of DS and daidzein to the vehicle-treatment group was almost comparable between the two doses (Table 4), suggesting that nonlinear disposition may not influence the effect of BCRP inhibitors. Conversely, lapatinib marginally increased plasma concentrations of ES and equol (Fig. 3, B and D), with a slight increase in their C_{max} and $AUC_{1\text{-}7h}$ values (Table 4). Thus, the inhibitory effect of lapatinib was more evident on the disposition of DS than ES.

Plasma Concentration of Isoflavone Sulfates in *Bcrp*$^{-/-}$ and Wild-Type Mice. Next, plasma concentrations of DS, GS, ES, and their parent isoflavones were measured in *Bcrp*$^{-/-}$ and wild-type mice to confirm the findings of the untargeted metabolomic analysis. DS, GS,

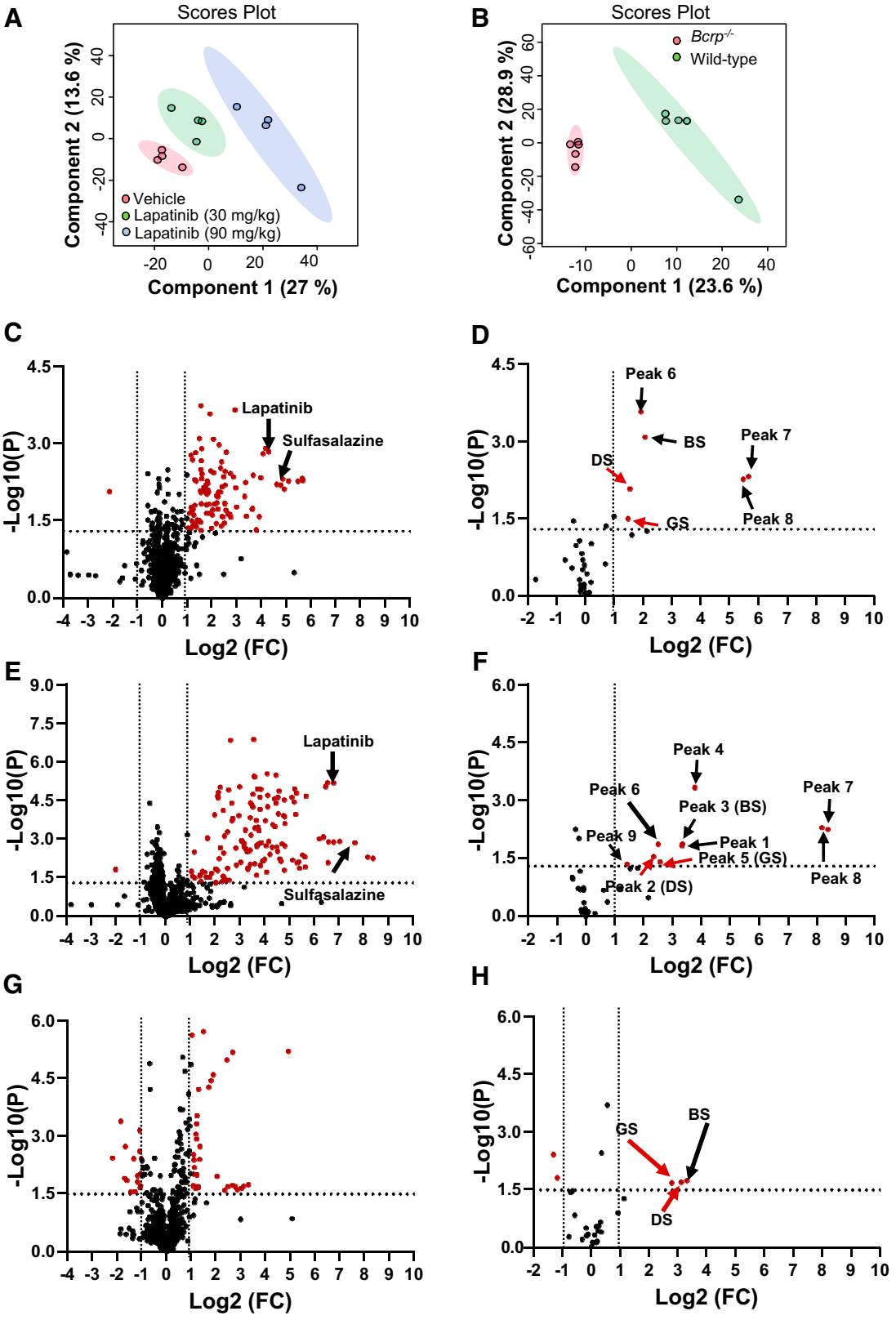

Fig. 1. Screening of BCRP substrates in the plasma of mice orally administered the BCRP inhibitor lapatinib (A, C–F) and in the plasma of *Bcrp*$^{-/-}$ mice (B, G–H). Wild-type mice were fed a diet containing 10% (w/w) soybean flour for 2 weeks; plasma samples were obtained 7 hours after oral administration of vehicle alone or lapatinib at 30 and 90 mg/kg. Plasma samples were obtained from wild-type and *Bcrp*$^{-/-}$ mice fed a normal diet. (A) and (B) represent PLS-DA score plots from peak intensities detected by untargeted metabolomics of plasma samples obtained from vehicle- and lapatinib-administered mice (A) and wild-type and *Bcrp*$^{-/-}$ mice (B). Circle areas indicate the 95% confidence intervals for each group. Volcano plots from peak intensities of vehicle- vs. lapatinib- (30 mg/kg) administered mice (C and D), vehicle- versus lapatinib- (90 mg/kg) administered mice (E and F), and wild-type versus *Bcrp*$^{-/-}$ mice (G and H) are shown. Fold changes (FC) were calculated by considering vehicle treatment (C–F) and wild-type mice (G and H) as the control group. All detected peaks are indicated in (C), (E), and (G), whereas selected peaks with neutral loss of 79.96 ± 0.01 Da after deconvolution of AIF-acquired data are plotted in (D), (F), and (H). The red dots indicate significantly increased peaks ($P < 0.05$, FC > 2).

TABLE 1
Compounds of interest in the metabolomic analysis of mice treated with or without lapatinib

Peak No.	Identity	Formula	Retention Time	Mass (*m/z*)			Fold Change		
				Theoretical	Observed [M-H]⁻	Error	Lapatinib administration		
							Lapatinib (30 mg/kg)	Lapatinib (90 mg/kg)	*Bcrp*$^{-/-}$
			min			*ppm*			
1	Unknown		2.45	—	196.051	—	4.67	10.7	—
2	DS	$C_{15}H_{10}O_7S$	3.45	333.014	333.023	27	2.91	5.06	8.7
3	BS[a]	$C_{16}H_{12}O_8S$	3.5	363.025	363.034	24	4.18	10.1	10
4	Unknown		3.6	—	546.986	—	4.47	13.6	—
5	GS	$C_{15}H_{10}O_8S$	3.66	349.009	349.017	22	2.78	5.94	6.9
6	Unknown		3.87	—	363.033	—	3.79	5.68	—
7	Debenzylated lapatinib (M1)-sulfate[a]	$C_{22}H_{21}N_4O_7S_2Cl^{35}$	4.13	551.046	551.07	43	50.0	332	—
8	Debenzylated lapatinib (M1)-sulfate[a]	$C_{22}H_{21}N_4O_7S_2Cl^{37}$	4.13	553.046	552.999	−84	44.4	288	—
9	Unknown		4.14	—	365.096	—	—	2.69	—

[a]Identification using authentic compounds has not yet been performed. Peaks #1, #4, #6, and #9 were structurally unidentified ions.

daidzein, and genistein were found at significantly higher plasma concentrations in *Bcrp*$^{-/-}$ mice than in wild-type mice, whereas plasma concentrations of ES did not differ between the two strains (Supplemental Fig. 1). A previous study showed differences in plasma concentrations of DS and GS between the two strains, but absolute concentration values were not reported (van de Wetering and Sapthu, 2012). Moreover, the plasma concentration of ES has not yet been reported.

Effect of Lapatinib on the Biliary and Urinary Excretion DS after Oral Administration of Its Parent Compound. BCRP is functionally expressed on the canalicular membranes of hepatocytes and brush-border membranes of renal proximal tubular cells. To evaluate the effect of lapatinib on biliary and urinary excretion of DS, the amounts of DS, daidzein, and DG excreted into the bile and urine were examined after oral administration of daidzein with or without lapatinib coadministration. Biliary excretion of DS was slightly decreased by oral administration of lapatinib (Supplemental Table 3), suggesting that lapatinib inhibited biliary excretion of DS. However, DS was found to be continuously excreted in bile even before administration of daidzein, which could be due to food-derived daidzein, which was converted to DS in the body. The amount of DS excretion until 1 hour after administration of daidzein was 2.5-fold higher than that before daidzein administration (Supplemental Table 3), but the increased amount of DS by daidzein administration was calculated to be at most 2.9% of dose. On the other hand, biliary excretion of DS at 2–3 and 3–4 hour was comparable to that at 0–1 hour (before daidzein administration). Thus, hepatic Bcrp may be also inhibited by lapatinib, but contribution of hepatic Bcrp and enterohepatic circulation to the change in plasma concentration profile of DS cannot be quantitatively estimated. In contrast, DS, DG, and daidzein were also excreted into the urine before and after oral administration of daidzein, but urinary excretion of DS was not significantly changed by oral administration of lapatinib (Supplemental Table 4).

Lapatinib and Febuxostat Increase Secretion of Isoflavone Sulfates into the Basal Side of Human iPS Cell-Derived Small Intestinal Epithelial-Like Cells. To demonstrate the effect of BCRP inhibitors on the intestinal disposition of isoflavone sulfates, the appearance of isoflavone sulfates on the basal side of human iPS cell-derived small intestinal epithelial-like cells was examined after the addition of their parent compounds to the apical side. These cells reportedly express BCRP on apical membranes and exhibit substrate basal-to-apical transport (Kodama et al., 2016). In the present study, parent isoflavones were first added to the apical chamber, and the appearance of their sulfates in the basal chamber was examined to mimic physiologic intestinal transport. DS, GS, and ES were detected in the basal chamber, and their appearance increased in a time-dependent manner (Fig. 4, A–C). The appearance of DS in the basal chamber was substantially higher than that of daidzein (Fig. 4, A and D). Lapatinib (1 μM) and febuxostat (10 μM) increased the amount of DS, GS, and ES (Fig. 4, A–C), whereas the levels of daidzein and genistein was not significantly affected (Fig. 4, D–E). In the basal chamber, the equol concentration was below the detection limit. LY was used as a paracellular marker, and lapatinib and febuxostat did not alter the permeability of LY (Fig. 4F). These results indicate the inhibition of intestinal BCRP by lapatinib and febuxostat, leading to an increased appearance of isoflavone sulfates on the basal side, which was consistent with the in vivo data (Figs. 2 and 3).

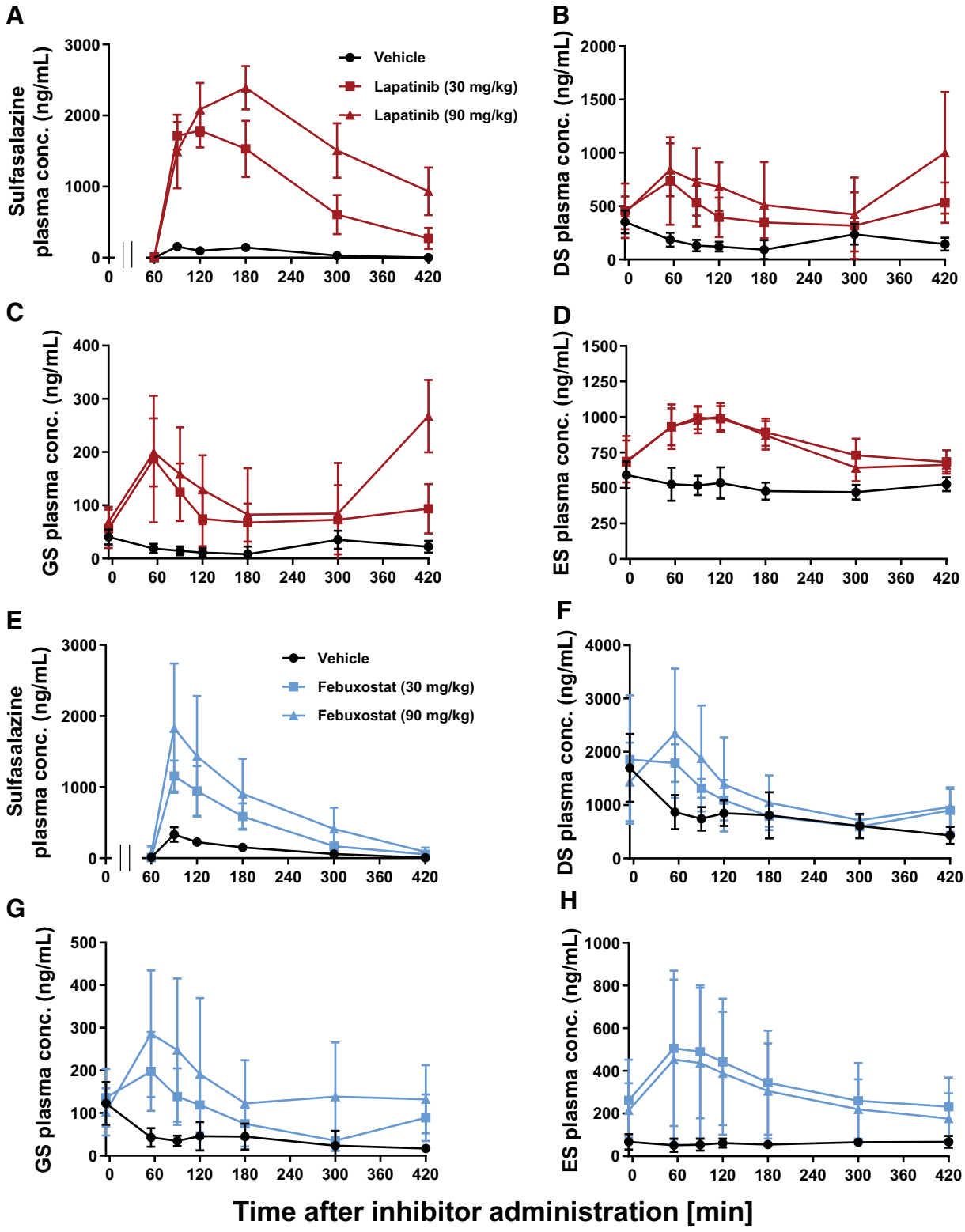

Fig. 2. Effect of oral administration of BCRP inhibitors (lapatinib and febuxostat) on plasma concentration-time profiles of sulfasalazine, DS, GS, and ES in mice fed a diet containing 10% (w/w) roasted soybean flour for 2 weeks. Sulfasalazine (5 mg/kg) was orally administered 1 hour after oral administration of lapatinib (10 and 30 mg/kg), febuxostat (10 and 30 mg/kg), or vehicle alone. Plasma samples were collected at designated times, and the concentrations of sulfasalazine (A and E), DS (B and F), GS (C and G), and ES (D and H) were measured by LC-MS/MS. Each value represents the mean ± S.D. (N = 4).

Lapatinib and Febuxostat Inhibit BCRP-Mediated Transport of DS and ES. The effect of lapatinib and febuxostat on the uptake of DS and ES in BCRP-expressing vesicles was examined to demonstrate the direct inhibition of BCRP-mediated transport of DS and ES by lapatinib and febuxostat. Although DS and ES are reportedly transported in BCRP-expressing membrane vesicles (van de Wetering and Sapthu,

TABLE 2

AUC ratios of isoflavone sulfates after oral administration of lapatinib in mice[a]

*P < 0.05; **P < 0.01, significantly different from the vehicle group (one-way ANOVA followed by Dunnett's post hoc test).

Compounds	Treatment	C_{max}	$AUC_{(0-7)}$	AUC Ratio
		ng/ml	*ng•h/ml*	
Sulfasalazine	Vehicle	$1.57 \times 10^2 \pm 0.36 \times 10^2$	$3.86 \times 10^2 \pm 1.08 \times 10^2$	–
	Lapatinib 30 mg/kg	$1.79 \times 10^3 \pm 0.24 \times 10^3$ **	$5.54 \times 10^3 \pm 1.39 \times 10^3$ **	14.4
	Lapatinib 90 mg/kg	$2.40 \times 10^3 \pm 3.05 \times 10^2$ **	$9.48 \times 10^3 \pm 1.79 \times 10^3$ **	24.5
DS	Vehicle	$3.52 \times 10^2 \pm 1.06 \times 10^2$	$1.24 \times 10^3 \pm 0.21 \times 10^3$	–
	Lapatinib 30 mg/kg	$7.37 \times 10^2 \pm 4.11 \times 10^2$	$3.09 \times 10^3 \pm 0.53 \times 10^3$ **	2.50
	Lapatinib 90 mg/kg	$1.00 \times 10^3 \pm 0.57 \times 10^3$	$4.40 \times 10^3 \pm 1.26 \times 10^3$ *	3.56
GS	Vehicle	$0.41 \times 10^2 \pm 0.14 \times 10^2$	$1.56 \times 10^2 \pm 0.45 \times 10^2$	–
	Lapatinib 30 mg/kg	$1.87 \times 10^2 \pm 1.19 \times 10^2$	$6.03 \times 10^2 \pm 1.40 \times 10^2$ **	3.86
	Lapatinib 90 mg/kg	$2.07 \times 10^2 \pm 1.33 \times 10^2$	$8.75 \times 10^2 \pm 2.49 \times 10^2$ *	5.60
ES	Vehicle	$5.92 \times 10^2 \pm 0.95 \times 10^2$	$3.58 \times 10^3 \pm 0.40 \times 10^3$	–
	Lapatinib 30 mg/kg	$9.95 \times 10^2 \pm 0.81 \times 10^2$ **	$5.84 \times 10^3 \pm 0.54 \times 10^3$ **	1.63
	Lapatinib 90 mg/kg	$1.00 \times 10^3 \pm 0.09 \times 10^3$ **	$5.62 \times 10^3 \pm 0.69 \times 10^3$ *	1.57

[a]Mean ± S.D. (n = 4).

2012), the inhibitory effects of lapatinib and febuxostat on transport by BCRP remain unknown. Membrane vesicles were prepared from Expi293F cells transfected with a plasmid encoding BCRP and exhibited ATP-dependent uptake of the typical substrate, LY (Fig. 5A). Both Ko143 (1 μM) and lapatinib (1 μM) decreased LY uptake (Fig. 5A), revealing that membrane vesicles functionally express BCRP. Furthermore, the uptake of DS and ES in BCRP-expressing vesicles was ATP-dependent (Fig. 5, B and C). The uptake of DS and ES was reduced in the presence of lapatinib, with IC_{50} values of 0.04 and 0.02 μM, respectively (Fig. 5, D and E). Furthermore, febuxostat inhibited the uptake of DS and ES, with IC_{50} values 0.09 μM and 0.05 μM, respectively; however, the inhibition potency of febuxostat was slightly lower than that of lapatinib ((Fig. 5, D and E).

As lapatinib inhibits P-gp and BCRP in vitro (Polli et al., 2008), P-gp–mediated uptake of isoflavone sulfates was examined. Membrane vesicles prepared from Expi293F cells transfected with a plasmid encoding P-gp exhibited ATP-dependent uptake of a typical substrate NMQ (Supplemental Fig. 4). In contrast, the uptake of DS and ES in P-gp–expressing vesicles was considerably low and unaltered by ATP (Supplemental Fig. 4), suggesting a minor role of P-gp in the transport of DS and ES.

Sulfate Conjugation of Isoflavones in Cytosolic Fractions Prepared from Mouse Small Intestine. Sulfotransferases (SULTs) are expressed in the small intestine and may also be affected by BCRP inhibitors. To examine this possibility, the effect of lapatinib and febuxostat on sulfate conjugation of isoflavones was examined in the cytosolic fraction of mouse small intestine. Lapatinib (0.1, 1, and 10 μM) and febuxostat (0.1, 1, and 10 μM) did not affect the formation of DS, GS, or ES (Supplemental Fig. 5), indicating that the BCRP inhibitors had little effect on the isoflavone sulfate conjugation in the small intestine.

Discussion

The present study revealed that oral administration of two BCRP inhibitors, lapatinib and febuxostat, increased plasma concentrations of DS, GS, and ES in mice fed a diet composed of phytoestrogens and their metabolites, with a concomitant increase in plasma concentration of the typical BCRP substrate sulfasalazine (Fig. 2). This indicates the vital role of BCRP in the disposition of isoflavone sulfates. This is in agreement with the finding that DS and GS were increased in the metabolomic analysis of plasma samples from *Bcrp*$^{-/-}$ mice, both in the present (Fig. 1F) and previous (van de Wetering and Sapthu, 2012) studies, and with the fact that DS and GS are increased in the plasma of *Bcrp*$^{-/-}$ mice after oral administration of daidzein and genistein (Álvarez et al., 2011; Yang et al., 2012). To the best of our knowledge, ours is the first study to demonstrate that plasma concentrations of DS and GS are rapidly altered by oral administration of BCRP inhibitors in mice. Gene knockout technology may alter the gene expression of

TABLE 3

AUC ratios of isoflavone sulfates after oral administration of febuxostat in mice[a]

*P < 0.05; **P < 0.01, significantly different from the vehicle group (one-way ANOVA followed by Dunnett's post hoc test).

Compounds	Treatment	C_{max}	$AUC_{(0-7)}$	AUC Ratio
		ng/ml	*ng•h/ml*	
Sulfasalazine	Vehicle	$3.34 \times 10^2 \pm 1.03 \times 10^2$	$6.07 \times 10^2 \pm 1.08 \times 10^2$	-
	Febuxostat 30 mg/kg	$1.16 \times 10^3 \pm 0.22 \times 10^3$	$2.27 \times 10^3 \pm 0.55 \times 10^3$	3.74
	Febuxostat 90 mg/kg	$1.83 \times 10^3 \pm 0.91 \times 10^3$ **	$3.80 \times 10^3 \pm 2.18 \times 10^3$ *	6.27
DS	Vehicle	$1.70 \times 10^3 \pm 0.64 \times 10^3$	$5.43 \times 10^3 \pm 1.76 \times 10^3$	–
	Febuxostat 30 mg/kg	$1.85 \times 10^3 \pm 1.20 \times 10^3$	$7.15 \times 10^3 \pm 0.92 \times 10^3$	1.32
	Febuxostat 90 mg/kg	$2.35 \times 10^3 \pm 1.22 \times 10^3$	$9.80 \times 10^3 \pm 5.44 \times 10^3$	1.80
GS	Vehicle	$1.22 \times 10^2 \pm 0.50 \times 10^2$	$2.79 \times 10^2 \pm 1.46 \times 10^2$	–
	Febuxostat 30 mg/kg	$1.98 \times 10^2 \pm 0.67 \times 10^2$	$6.59 \times 10^2 \pm 0.84 \times 10^2$	2.36
	Febuxostat 90 mg/kg	$2.86 \times 10^2 \pm 1.48 \times 10^2$	$1.15 \times 10^3 \pm 0.73 \times 10^3$ *	4.11
ES	Vehicle	$0.67 \times 10^2 \pm 0.36 \times 10^2$	$4.28 \times 10^2 \pm 0.76 \times 10^2$	–
	Febuxostat 30 mg/kg	$5.06 \times 10^2 \pm 3.64 \times 10^2$	$2.39 \times 10^3 \pm 1.59 \times 10^3$	5.60
	Febuxostat 90 mg/kg	$4.53 \times 10^2 \pm 3.75 \times 10^2$	$2.07 \times 10^3 \pm 1.48 \times 10^3$	4.83

[a]Mean ± S.D. (n = 4).

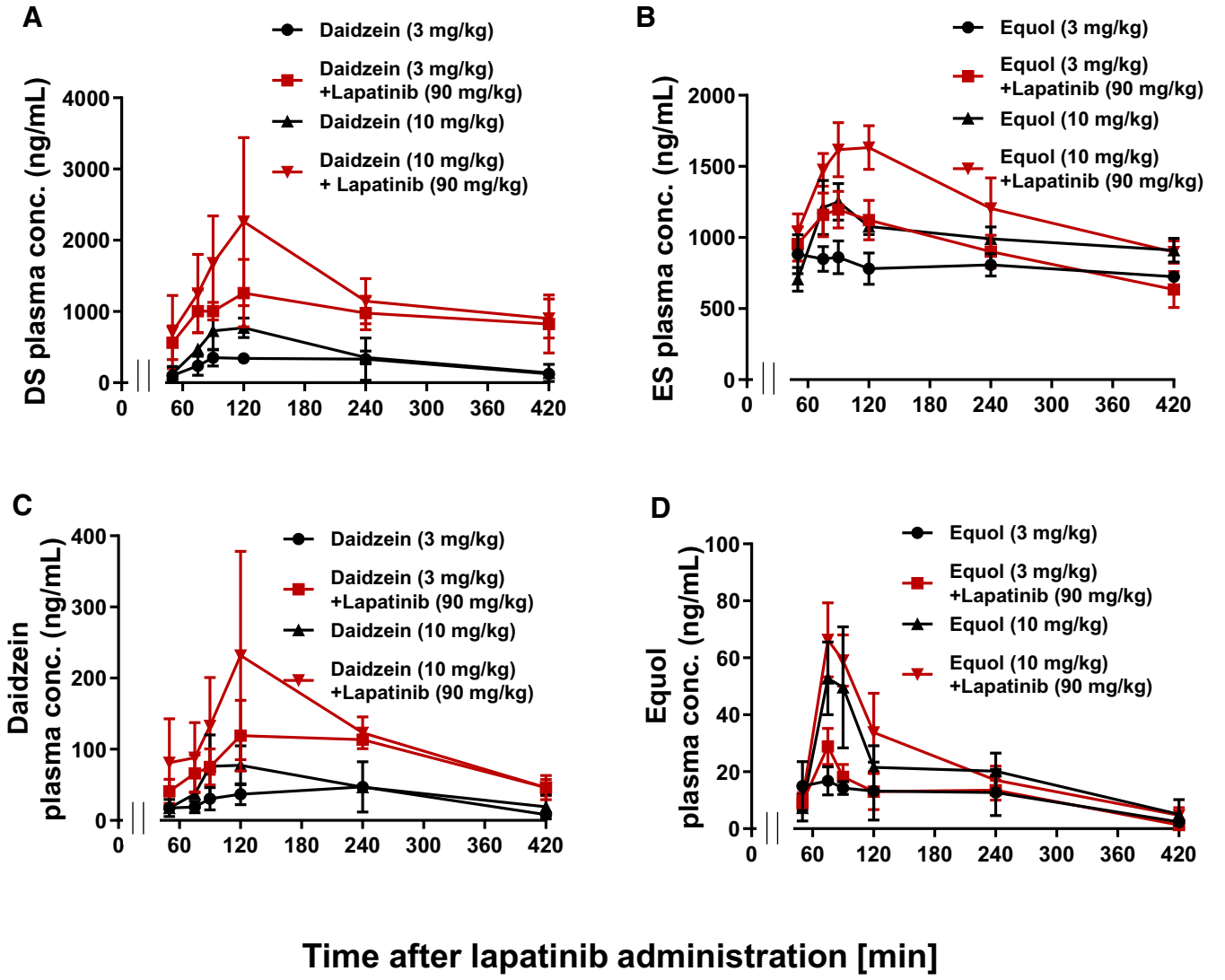

Fig. 3. Effects of oral administration of lapatinib on plasma concentration-time profiles of DS and ES in mice after oral administration of daidzein and equol. Daidzein (3 or 10 mg/kg) or equol (3 or 10 mg/kg) was orally administered 1 hour after oral administration of lapatinib (90 mg/kg) or vehicle alone. Plasma samples were collected at designated times, and the concentrations of DS (A), ES (B), daidzein (C), and equol (D) were measured by LC-MS/MS. Each value represents the mean ± S.D. (N = 4).

transporters and metabolic enzymes other than the target as a secondary effect. Indeed, mRNA levels of drug-metabolizing enzymes, such as catechol-*O*-methyltransferase, have been compensated in *Bcrp* knockout rats (Zamek-Gliszczynski et al., 2013). Therefore, the preset study is the first to include in vivo inhibition experiments using BCRP inhibitors to undertake an untargeted metabolomic approach to identify biomarkers of BCRP inhibition.

BCRP is expressed in various organs and extrudes substrates from cells in the small intestine, renal proximal tubules, and hepatic bile ducts. In the small intestine, BCRP may hinder the absorption of various substrate drugs (Keskitalo et al., 2009; Mizuno et al., 2012; Gotanda et al., 2015). BCRP is coexpressed with SULT in the gastrointestinal region, especially in the lower part of the small intestine, playing a vital role in the intestinal disposition of 4-methylumbelliferone sulfate (Enokizono et al., 2007b). To examine the role of BCRP in the disposition of DS, GS, and ES, we examined the appearance of these compounds in the basal chamber of human iPS cell-derived small intestinal epithelial-like cells and observed a significant increase in the presence of these BCRP inhibitors (Fig. 4, A–C); this may indicate that BCRP might inhibit intestinal secretion of these isoflavone sulfates and their parent compounds. Both SULT and BCRP are functionally expressed in small intestinal cells derived from human iPS cells (Iwao et al., 2015; Kodama et al., 2016). Therefore, it can be speculated that cooperation between drug-metabolizing enzymes and transporters could be observed in the cells as illustrated in Fig 6. This is in agreement with the present finding that BCRP inhibition increased the basal side appearance of sulfate conjugates after adding parent compounds on the apical side (Fig. 4). Yang et al. (2012) reported an increase in GS in the basolateral chamber in the presence of Ko143, a typical inhibitor of BCRP, after the addition of genistein to the apical chamber of Caco-2 cells. However, it should be noted that other efflux transporters may be expressed and may play a role in the basolateral excretion of DS, GS, and ES in human iPS cell-derived small intestinal cells. Recently, P-gp–knockout human iPS cell-derived small intestinal epithelial-like cells were established using genome editing technologies (Ichikawa et al., 2021). The combination of genome editing and iPS differentiation technologies

TABLE 4

AUC ratios of DS and ES after oral administration of each parent compound in the presence of lapatinib in mice[a]

*P < 0.05; **P < 0.01, significantly different from the vehicle group (Student's t test).

Dose	Compound	Treatment	C_{max}	$AUC_{(1-7)}$	AUC Ratio
			ng/ml	*ng•h/ml*	
Daidzein 3 mg/kg	Daidzein	Vehicle	$0.47 \times 10^2 \pm 0.36 \times 10^2$	$1.98 \times 10^2 \pm 0.96 \times 10^2$	-
		Lapatinib	$1.19 \times 10^2 \pm 0.49 \times 10^2$	$5.60 \times 10^2 \pm 0.75 \times 10^2$ *	2.83
	DS	Vehicle	$3.51 \times 10^2 \pm 1.18 \times 10^2$	$1.61 \times 10^3 \pm 0.81 \times 10^3$	-
		Lapatinib	$1.26 \times 10^3 \pm 0.47 \times 10^3$ **	$6.08 \times 10^3 \pm 0.88 \times 10^3$ **	3.77
Daidzein 10 mg/kg	Daidzein	Vehicle	$0.77 \times 10^2 \pm 0.28 \times 10^2$	$2.87 \times 10^2 \pm 0.83 \times 10^2$	-
		Lapatinib	$2.32 \times 10^2 \pm 1.47 \times 10^2$	$7.62 \times 10^2 \pm 2.01 \times 10^2$ **	2.65
	DS	Vehicle	$7.70 \times 10^2 \pm 1.39 \times 10^2$	$2.50 \times 10^3 \pm 0.49 \times 10^3$	-
		Lapatinib	$2.26 \times 10^3 \pm 1.18 \times 10^3$ *	$8.23 \times 10^3 \pm 1.49 \times 10^3$ **	3.28
Equol 3 mg/kg	Equol	Vehicle	$0.16 \times 10^2 \pm 0.05 \times 10^2$	$0.66 \times 10^2 \pm 0.22 \times 10^2$	-
		Lapatinib	$0.78 \times 10^2 \pm 0.50 \times 10^2$	$1.31 \times 10^2 \pm 0.22 \times 10^2$	1.98
	ES	Vehicle	$8.82 \times 10^3 \pm 0.14 \times 10^3$	$4.87 \times 10^3 \pm 0.19 \times 10^3$	-
		Lapatinib	$1.20 \times 10^3 \pm 0.13 \times 10^3$ *	$5.64 \times 10^3 \pm 0.60 \times 10^3$	1.15
Equol 10 mg/kg	Equol	Vehicle	$0.28 \times 10^2 \pm 0.06 \times 10^2$	$0.68 \times 10^2 \pm 0.14 \times 10^2$	-
		Lapatinib	$1.05 \times 10^2 \pm 0.77 \times 10^2$	$1.51 \times 10^2 \pm 0.20 \times 10^2$	1.66
	ES	Vehicle	$1.25 \times 10^3 \pm 0.13 \times 10^3$	$6.21 \times 10^3 \pm 0.11 \times 10^3$	-
		Lapatinib	$1.63 \times 10^3 \pm 0.15 \times 10^3$ **	$7.71 \times 10^3 \pm 0.79 \times 10^3$ **	1.24

[a]Mean ±S.D. (n = 4).

may provide an in-depth understanding of the role of BCRP and other transporters in the intestinal transport of isoflavone sulfates.

In the present study, the C_{max} values of lapatinib and febuxostat after oral administration (90 mg/kg) (Supplemental Fig. 3) were almost comparable to their clinical concentrations (Chu et al., 2008; Miyata et al., 2016). Therefore, changes in the disposition of BCRP substrates after oral administration (Figs. 2 and 3) may imply that lapatinib and febuxostat may also inhibit BCRP in humans. Febuxostat has been

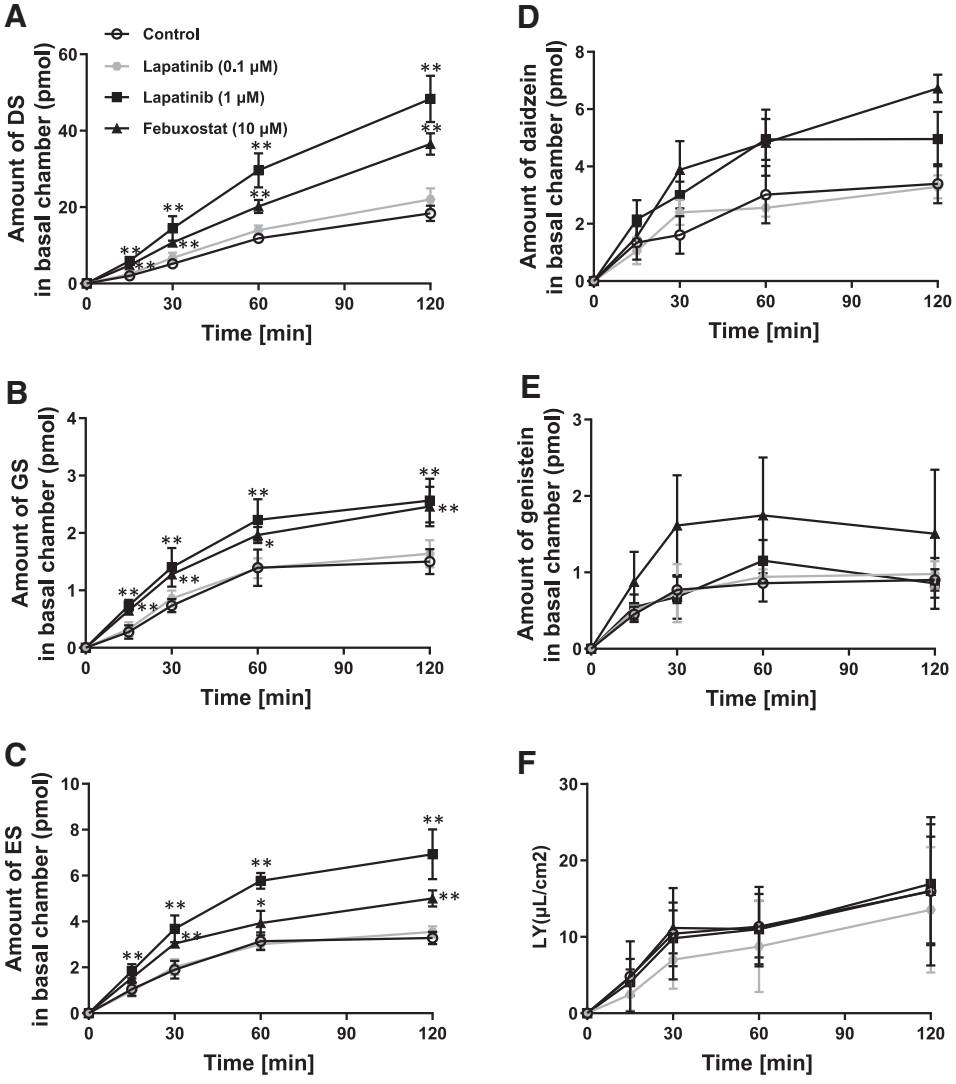

Fig. 4. Daidzein, genistein, and their sulfate conjugates in the basal chamber of human iPS cell-derived small intestinal epithelial cells and inhibition by lapatinib and febuxostat. A mixture of daidzein, genistein, equol (1 μM each), and LY (100 μM) was applied to the apical chamber in the absence (open circles) or presence of lapatinib (0.1 μM, gray diamonds; 1 μM, closed squares) or febuxostat (10 μM, closed triangles). Aliquots of the buffer in the basal chamber were collected at designated times, and concentrations of each compound were measured by LC-MS/MS. DS (A), GS (B), ES (C), daidzein (D), and genistein (E) in basal chambers are shown. Equol was present under the detection limit (<6 pmol). Permeation of LY is shown in panel (F) to assess membrane integrity. Each value represents the mean ± S.D. (N = 4). *P < 0.05; **P < 0.01, significantly different from the vehicle control (one-way ANOVA followed by Dunnett's post hoc test).

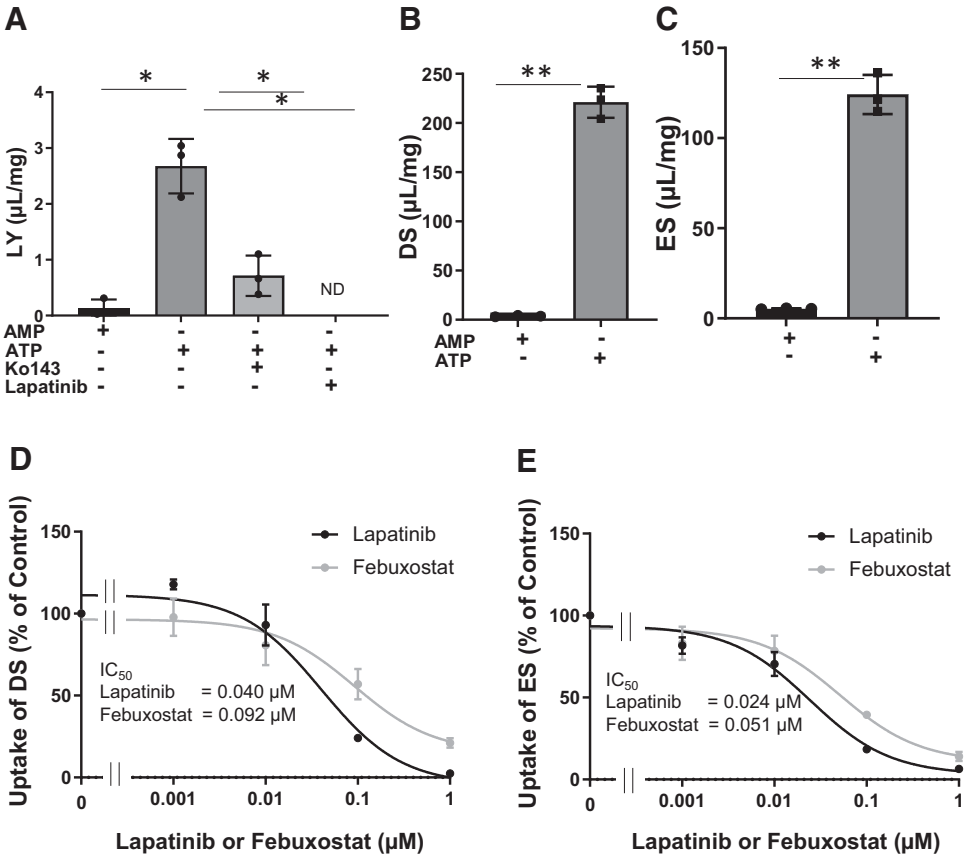

Fig. 5. Inhibitory effect of lapatinib and febuxostat on uptake of DS and ES in BCRP-expressing membrane vesicles. Uptake of LY (10 μM; A), DS (3 μM; B), and ES (3 μM; C) was measured in membrane vesicles prepared from Expi293F cells transiently transfected with a plasmid encoding BCRP in the absence and presence of ATP. Uptake of DS (D) and ES (E) in the BCRP-expressing vesicles was measured in the presence of various concentrations of lapatinib (black circles) and febuxostat (gray circles). Vesicles were incubated for 5 minutes with LY, DS, and ES, and a diluted aliquot was quickly applied to a spin column to terminate the uptake. Each value represents the mean ± S.D. (N = 3–4). *P < 0.05; **P < 0.01, significantly different between each group [one-way ANOVA followed by Dunnett's post hoc test (A), Student's t test (B and C)].

reported to significantly increase the AUC values of rosuvastatin in humans (Lehtisalo et al., 2020). In contrast, sulfate conjugates, such as DS and GS, have been detected in 10%–20% of total metabolites after soybean consumption in humans (Hosoda et al., 2011; Soukup et al., 2016; Obara et al., 2019). In the present study, both DS and GS were detected in the plasma of mice fed roasted soybean flour and were increased after oral administration of BCRP inhibitors (Fig. 2). These observations imply that DS and GS can be detected in the circulating plasma of humans under appropriate dietary conditions and can be used to evaluate BCRP inhibition after oral administration of inhibitor drugs. However, there are considerable differences in the metabolism of isoflavones in humans as compared with mice, with the predominant metabolites of daidzein and genistein occurring as mixed conjugates and sulfoglucuronides in humans (Soukup et al., 2016), whereas the major daidzein and genistein metabolites in mice are monoglucuronides and monosulfate conjugates. The involvement of such metabolic pathways in the systemic elimination of isoflavones may hinder the appropriate estimation of BCRP inhibition and should be further validated.

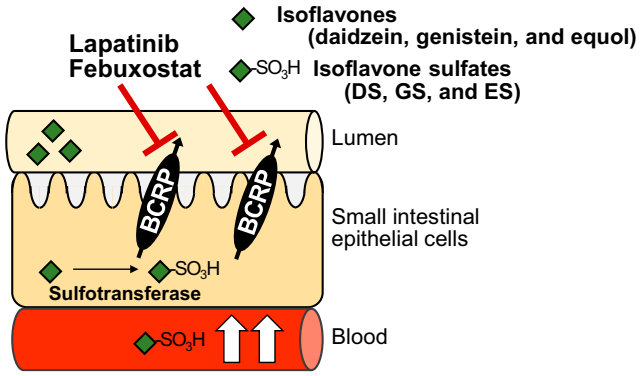

Fig. 6. Schematic illustration representing inhibition of intestinal Bcrp-mediated transport of isoflavone sulfates by Bcrp inhibitors. Orally taken isoflavones (daidzein and genistein) are absorbed by intestinal epithelial cells and then further metabolized by sulfotransferase to form DS and GS, respectively. The presence of BCRP inhibitors lapatinib and febuxostat prevents transport of these isoflavone sulfates back to the intestinal lumen by BCRP, leading to elevation of DS and GS in the plasma.

In the present study, ES was found to be a suitable substrate for BCRP in vitro (Fig. 5C); however, it was not selected as a significantly increased ion peak in animals treated with BCRP inhibitors or with the *Bcrp* gene knockout (Fig. 1, D, F and H). The plasma concentration of ES in *Bcrp*$^{-/-}$ plasma was comparable to that of wild-type mice (Supplemental Fig. 1C). A previous targeted metabolomic study revealed that ion peaks of DS and GS in plasma samples of *Bcrp*$^{-/-}$ mice were higher than those in wild-type mice, whereas ES did not exhibit differences between *Bcrp*$^{-/-}$ and wild-type mice (van de Wetering and Sapthu, 2012). However, in our study, the plasma concentration profile of ES was found to be increased after oral administration of both lapatinib and febuxostat (Figs. 2 and 3). Such discrepancies between the screening and confirmation processes may be attributed to the relatively rapid elimination of ES from the body, which could hinder the use of ES as a biomarker of BCRP inhibition when collecting plasma samples in the late phase after ingestion of isoflavone-containing foods.

The utilization of food-derived compounds has been proposed to assess transporter-mediated DDIs. For instance, taurine has been used to assess OAT1 inhibition (Tsuruya et al., 2016). This strategy may

afford additional advantages when compared with a probe substrate, allowing the early evaluation of DDI risks during drug development. Chu et al. (2018) discussed several criteria for ideal biomarkers for drug transporters. These are partially valid for DS and GS, given that their in vitro transport by BCRP was characterized in the present study (Figs. 4 and 5) as well as in previous reports (van de Wetering and Sapthu, 2012; Yang et al., 2012). Furthermore, DS and GS exhibited a ratio of area under the plasma concentration-time profile ≥ 2 in *Bcrp*$^{-/-}$ mice (Supplemental Fig. 1) and in the presence of BCRP inhibitors (Tables 2 and 3), suggesting that these compounds have the potential to be used as biomarkers for BCRP inhibition. However, the ratio of area under the plasma concentration-time of DS and GS was lower than that of a typical BCPR substrate sulfasalazine, showing limited sensitivity of these compounds as biomarkers. In addition, these compounds are food-derived, and their plasma concentrations may be highly affected by background factors, including food intake. This point may not be compatible with the criteria proposed by Chu et al. (2018). It should be noted that food-derived compounds may be difficult to detect in the plasma without the ingestion of a specialized diet. Interindividual variations in the intake of food-derived compounds and their precursors may also affect absolute values of plasma concentrations. To overcome these limitations, intake of the respective food should be strictly controlled. In humans, isoflavone sulfates have a relatively short half-life in plasma: approximately 3 hours for DS and 6 hours for GS (Shelnutt et al., 2002). Therefore, their plasma concentrations are primarily affected by food intake. Another concern is the interindividual differences in microbiota, as equol can be produced by intestinal bacteria from daidzein (Kim, 2015). Therefore, normalization of plasma concentrations of these compounds using blank plasma may be essential for the quantitative estimation of their AUC values.

In conclusion, this is the first report proposing the use of isoflavone sulfates, DS and GS, after appropriate food intake, to evaluate changes in BCRP activity in vivo, with increased plasma concentration after oral administration of BCRP inhibitors. Although the present findings are valid in rodents, the evaluation of inhibitory effects of new investigational drugs on BCRP in preclinical studies using DS, GS, and ES as physiologic BCRP substrates, may help elucidate potential BCRP-mediated DDIs. Further studies are needed to elucidate the validity of this strategy in clinical investigations of potential BCRP-mediated DDIs.

Acknowledgments

The authors thank Hirofumi Yagi (Laboratory of Molecular Pharmacotherapeutics, Kanazawa University, Japan) for his contribution to the in vivo mouse studies. The authors would also like to thank Dr. Masahiko Ito and Dr. Shinji Mima at the Research and Development Management Headquarters, FUJIFILM Corporation, Japan, for fruitful discussions regarding human iPS cell-derived small intestinal epithelial-like cells.

Authorship Contributions

Participated in research design: Agustina, Masuo, Kido, Shinoda, Kato.

Conducted experiments: Agustina, Masuo, Kido, Shinoda.

Performed data analysis: Agustina, Masuo, Shinoda.

Wrote or contributed to writing the manuscript: Agustina, Masuo, Kido, Ishimoto, Kato.

References

Álvarez AI, Vallejo F, Barrera B, Merino G, Prieto JG, Tomás-Barberán F, and Espín JC (2011) Bioavailability of the glucuronide and sulfate conjugates of genistein and daidzein in breast cancer resistance protein 1 knockout mice. *Drug Metab Dispos* **39**:2008–2012.

An G and Morris ME (2011) The sulfated conjugate of biochanin A is a substrate of breast cancer resistant protein (ABCG2). *Biopharm Drug Dispos* **32**:446–457.

Chong J, Wishart DS, and Xia J (2019) Using MetaboAnalyst 4.0 for comprehensive and integrative metabolomics data analysis. *Curr Protoc Bioinforma* **68**.

Chu QSC, Cianfrocca ME, Goldstein LJ, Gale M, Murray N, Loftiss J, Arya N, Koch KM, Pandite L, Fleming RA, et al. (2008) A phase I and pharmacokinetic study of lapatinib in combination with letrozole in patients with advanced cancer. *Clin Cancer Res* **14**:4484–4490.

Chu X, Liao M, Shen H, Yoshida K, Zur AA, Arya V, Galetin A, Giacomini KM, Hanna I, Kusuhara H, et al.; International Transporter Consortium (2018) Clinical probes and endogenous biomarkers as substrates for transporter drug-drug interaction evaluation: perspectives from the International Transporter Consortium. *Clin Pharmacol Ther* **104**:836–864.

Enokizono J, Kusuhara H, and Sugiyama Y (2007a) Effect of breast cancer resistance protein (Bcrp/Abcg2) on the disposition of phytoestrogens. *Mol Pharmacol* **72**:967–975.

Enokizono J, Kusuhara H, and Sugiyama Y (2007b) Regional expression and activity of breast cancer resistance protein (Bcrp/Abcg2) in mouse intestine: overlapping distribution with sulfotransferases. *Drug Metab Dispos* **35**:922–928.

Gotanda K, Tokumoto T, Hirota T, Fukae M, and Ieiri I (2015) Sulfasalazine disposition in a subject with 376C>T (nonsense mutation) and 421C>A variants in the ABCG2 gene. *Br J Clin Pharmacol* **80**:1236–1237.

Harvey RD, Aransay NR, Isambert N, Lee J-S, Arkenau T, Vansteenkiste J, Dickinson PA, Bui K, Weilert D, So K, et al. (2018) Effect of multiple-dose osimertinib on the pharmacokinetics of simvastatin and rosuvastatin. *Br J Clin Pharmacol* **84**:2877–2888.

Hosoda K, Furuta T, and Ishii K (2011) Metabolism and disposition of isoflavone conjugated metabolites in humans after ingestion of kinako. *Drug Metab Dispos* **39**:1762–1767.

Ichida K, Matsuo H, Takada T, Nakayama A, Murakami K, Shimizu T, Yamanashi Y, Kasuga H, Nakashima H, Nakamura T, et al. (2012) Decreased extra-renal urate excretion is a common cause of hyperuricemia. *Nat Commun* **3**:764.

Ichikawa M, Negoro R, Kawai K, Yamashita T, Takayama K, and Mizuguchi H (2021) Vinblastine treatment decreases the undifferentiated cell contamination of human iPSC-derived intestinal epithelial-like cells. *Mol Ther Methods Clin Dev* **20**:463–472.

Iwao T, Kodama N, Kondo Y, Kabeya T, Nakamura K, Horikawa T, Niwa T, Kurose K, and Matsunaga T (2015) Generation of enterocyte-like cells with pharmacokinetic functions from human induced pluripotent stem cells using small-molecule compounds. *Drug Metab Dispos* **43**:603–610.

Jonker JW, Buitelaar M, Wagenaar E, Van Der Valk MA, Scheffer GL, Scheper RJ, Plosch T, Kuipers F, Elferink RP, Rosing H, et al. (2002) The breast cancer resistance protein protects against a major chlorophyll-derived dietary phototoxin and protoporphyria. *Proc Natl Acad Sci USA* **99**:15649–15654.

Kabeya T, Mima S, Imakura Y, Miyashita T, Ogura I, Yamada T, Yasujima T, Yuasa H, Iwao T, and Matsunaga T (2020) Pharmacokinetic functions of human induced pluripotent stem cell-derived small intestinal epithelial cells. *Drug Metab Pharmacokinet* **35**:374–382.

Keskitalo JE, Zolk O, Fromm MF, Kurkinen KJ, Neuvonen PJ, and Niemi M (2009) ABCG2 polymorphism markedly affects the pharmacokinetics of atorvastatin and rosuvastatin. *Clin Pharmacol Ther* **86**:197–203.

Kim D-H (2015) Gut microbiota-mediated drug-antibiotic interactions. *Drug Metab Dispos* **43**:1581–1589.

Kobayashi Y, Fukami T, Nakajima A, Watanabe A, Nakajima M, and Yokoi T (2012) Species differences in tissue distribution and enzyme activities of arylacetamide deacetylase in human, rat, and mouse. *Drug Metab Dispos* **40**:671–679.

Kodama N, Iwao T, Katano T, Ohta K, Yuasa H, and Matsunaga T (2016) Characteristic analysis of intestinal transport in enterocyte-like cells differentiated from human induced pluripotent stem cells. *Drug Metab Dispos* **44**:1662–1667.

Lafaye A, Junot C, Ramounet-Le Gall B, Fritsch P, Ezan E, and Tabet JC (2004) Profiling of sulfoconjugates in urine by using precursor ion and neutral loss scans in tandem mass spectrometry. Application to the investigation of heavy metal toxicity in rats. *J Mass Spectrom* **39**:655–664.

Lai Y, Mandlekar S, Shen H, Holenarsipur VK, Langish R, Rajanna P, Murugesan S, Gaud N, Selvam S, Date O, et al. (2016) Coproporphyrins in plasma and urine can be appropriate clinical biomarkers to recapitulate drug-drug interactions mediated by organic anion transporting polypeptide inhibition. *J Pharmacol Exp Ther* **358**:397–404.

Lee CA, O'Connor MA, Ritchie TK, Galetin A, Cook JA, Ragueneau-Majlessi I, Ellens H, Feng B, Taub ME, Paine MF, et al. (2015) Breast cancer resistance protein (ABCG2) in clinical pharmacokinetics and drug interactions: practical recommendations for clinical victim and perpetrator drug-drug interaction study design. *Drug Metab Dispos* **43**:490–509.

Lehtisalo M, Keskitalo JE, Tornio A, Lapatto-Reiniluoto O, Deng F, Jaatinen T, Viinamäki J, Neuvonen M, Backman JT, and Niemi M (2020) Febuxostat, but not allopurinol, markedly raises the plasma concentrations of the breast cancer resistance protein substrate rosuvastatin. *Clin Transl Sci* **13**:1236–1243.

Mao Q and Unadkat JD (2015) Role of the breast cancer resistance protein (BCRP/ABCG2) in drug transport–an update. *AAPS J* **17**:65–82.

Miyata H, Takada T, Toyoda Y, Matsuo H, Ichida K, and Suzuki H (2016) Identification of febuxostat as a new strong ABCG2 inhibitor: potential applications and risks in clinical situations. *Front Pharmacol* **7**:518.

Mizuno T, Fukudo M, Terada T, Kamba T, Nakamura E, Ogawa O, Inui K, and Katsura T (2012) Impact of genetic variation in breast cancer resistance protein (BCRP/ABCG2) on sunitinib pharmacokinetics. *Drug Metab Pharmacokinet* **27**:631–639.

Nardone-White DT, Bissada JE, Abouda AA, and Jackson KD (2021) Detoxication versus bioactivation pathways of lapatinib in vitro: UGT1A1 catalyzes the hepatic glucuronidation of debenzylated lapatinib. *Drug Metab Dispos* **49**:233–244.

Obara A, Kinoshita M, Hosoda K, Yokokawa A, Shibasaki H, and Ishii K (2019) Identification of equol-7-glucuronide-4′-sulfate, monoglucuronides and monosulfates in human plasma of 2 equol producers after administration of *kinako* by LC-ESI-MS. *Pharmacol Res Perspect* **7**:e00478.

Omote H and Moriyama Y (2018) Reconstitution and transport analysis of eukaryotic transporters in the post-genomic era. *Methods Mol Biol* **1700**:343–352.

Polli JW, Humphreys JE, Harmon KA, Castellino S, O'Mara MJ, Olson KL, John-Williams LS, Koch KM, and Serabjit-Singh CJ (2008) The role of efflux and uptake transporters in [N-{3-chloro-4-[(3-fluorobenzyl)oxy]phenyl}-6-[5-({[2-(methylsulfonyl)ethyl]amino}methyl)-2-furyl]-4-quinazolinamine (GW572016, lapatinib) disposition and drug interactions. *Drug Metab Dispos* **36**:695–701.

Shelnutt SR, Cimino CO, Wiggins PA, Ronis MJJ, and Badger TM (2002) Pharmacokinetics of the glucuronide and sulfate conjugates of genistein and daidzein in men and women after consumption of a soy beverage. *Am J Clin Nutr* **76**:588–594.

Soukup ST, Helppi J, Müller DR, Zierau O, Watzl B, Vollmer G, Diel P, Bub A, and Kulling SE (2016) Phase II metabolism of the soy isoflavones genistein and daidzein in humans, rats and mice: a cross-species and sex comparison. *Arch Toxicol* **90**:1335–1347.

Tada I, Chaleckis R, Tsugawa H, Meister I, Zhang P, Lazarinis N, Dahlén B, Wheelock CE, and Arita M (2020) Correlation-based deconvolution (CorrDec) to generate high-quality MS2 spectra from data-independent acquisition in multisample studies. *Anal Chem* **92**:11310–11317.

Tsugawa H, Nakabayashi R, Mori T, Yamada Y, Takahashi M, Rai A, Sugiyama R, Yamamoto H, Nakaya T, Yamazaki M, et al. (2019) A cheminformatics approach to characterize metabolomes in stable-isotope-labeled organisms. *Nat Methods* **16**:295–298.

Tsuruya Y, Kato K, Sano Y, Imamura Y, Maeda K, Kumagai Y, Sugiyama Y, and Kusuhara H (2016) Investigation of endogenous compounds applicable to drug-drug interaction studies involving the renal organic anion transporters, OAT1 and OAT3, in humans. *Drug Metab Dispos* **44**:1925–1933.

van de Wetering K and Sapthu S (2012) ABCG2 functions as a general phytoestrogen sulfate transporter in vivo. *FASEB J* **26**:4014–4024.

van Herwaarden AE, Wagenaar E, Merino G, Jonker JW, Rosing H, Beijnen JH, and Schinkel AH (2007) Multidrug transporter ABCG2/breast cancer resistance protein secretes riboflavin (vitamin B2) into milk. *Mol Cell Biol* **27**:1247–1253.

Vlaming MLH, Lagas JS, and Schinkel AH (2009) Physiological and pharmacological roles of ABCG2 (BCRP): recent findings in Abcg2 knockout mice. *Adv Drug Deliv Rev* **61**:14–25.

Yang Z, Zhu W, Gao S, Yin T, Jiang W, and Hu M (2012) Breast cancer resistance protein (ABCG2) determines distribution of genistein phase II metabolites: reevaluation of the roles of ABCG2 in the disposition of genistein. *Drug Metab Dispos* **40**:1883–1893.

Yasuda K, Ganguly S, and Schuetz EG (2018) Pheophorbide A: fluorescent Bcrp substrate to measure oral drug-drug interactions in real time in vivo. *Drug Metab Dispos* **46**:dmd.118.083584.

Zamek-Gliszczynski MJ, Goldstein KM, Paulman A, Baker TK, and Ryan TP (2013) Minor compensatory changes in SAGE Mdr1a (P-gp), Bcrp, and Mrp2 knockout rats do not detract from their utility in the study of transporter-mediated pharmacokinetics. *Drug Metab Dispos* **41**:1174–1178.

Address correspondence to: Dr. Yukio Kato, Faculty of Pharmacy, Kanazawa University, Kakuma-machi, Kanazawa 920-1192, Japan. E-mail: ykato@p.kanazawa-u.ac.jp

Title
Identification of Food-derived Isoflavone Sulfates as Inhibition Markers for Intestinal Breast Cancer Resistance Proteins

Article's Authors
Rina Agustina, Yusuke Masuo, Yasuto Kido, Kyosuke Shinoda, Takahiro Ishimoto, and Yukio Kato

Journal Title
Drug Metabolism & Disposition

Manuscript Number
DMD-AR-2021-000534

Supplemental Information

Supplementary Table 1
Bioanalytical analysis validation[a]

Compounds	LLOQ nM	Concentration nM	Accuracy %	Precision %
Daidzein	1	30	-2.01 -6.33 -12	9.58
Genistein	1	30	1.77 6.6 -11.6	9.48
Equol	800	3000	-5.33 6.67 -12.6	9.76
DS	1	30	-10 -1.33 2.67	6.48
GS	1	30	6 8.77 -11.6	9.45
ES	1	30	-6.67 -2.33 1.67	4.17

[a]Accuracy and precision was calculated from one concentration (N = 3).

Supplementary Table 2
AUC ratios of isoflavones after oral administration of lapatinib and febuxostat in mice fed a diet containing 10% (w/w) roasted soybean flour for 2 weeks[a]

Compounds	Treatment	C_{max} (ng/mL)	$AUC_{(0-7)}$ (ng•h/mL)	AUC Ratio
Daidzein	Vehicle	$0.33\times10^2\pm0.14\times10^2$	$1.27\times10^2\pm0.26\times10^2$	-
	Lapatinib 30 mg/kg	$0.78\times10^2\pm0.42\times10^{2\,*}$	$2.94\times10^2\pm0.54\times10^{2\,*}$	2.33
	Lapatinib 90 mg/kg	$0.79\times10^2\pm0.16\times10^{2\,**}$	$4.05\times10^2\pm1.01\times10^{2\,**}$	3.21
Genistein	Vehicle	$0.34\times10^2\pm0.14\times10^2$	$0.72\times10^2\pm0.12\times10^2$	-
	Lapatinib 30 mg/kg	$1.70\times10^2\pm1.01\times10^{2\,*}$	$2.35\times10^2\pm0.75\times10^{2\,**}$	3.24
	Lapatinib 90 mg/kg	$2.10\times10^2\pm0.47\times10^{2\,**}$	$3.27\times10^2\pm0.64\times10^{2\,**}$	4.51
Equol	Vehicle	N.D.	N.D.	
	Lapatinib 30 mg/kg	N.D.	N.D.	
	Lapatinib 90 mg/kg	N.D.	N.D.	
Daidzein	Vehicle	$0.80\times10^2\pm0.23\text{x}10^2$	$2.43\times10^2\pm0.71\times10^2$	-
	Febuxostat 30 mg/kg	$0.74\times10^2\pm0.19\text{x}10^2$	$2.77\times10^2\pm0.35\times10^2$	1.14
	Febuxostat 90 mg/kg	$0.59\times10^2\pm0.28\text{x}10^2$	$3.15\times10^2\pm1.57\times10^2$	1.29
Genistein	Vehicle	$0.24\times10^2\pm0.05\text{x}10^2$	$0.81\times10^2\pm0.21\times10^2$	-
	Febuxostat 30 mg/kg	$0.31\times10^2\pm0.17\text{x}10^2$	$1.04\times10^2\pm0.06\times10^2$	1.30
	Febuxostat 90 mg/kg	$0.25\times10^2\pm0.08\times10^2$	$1.34\times10^2\pm0.58\times10^2$	1.67
Equol	Vehicle	N.D.	N.D.	
	Febuxostat 30 mg/kg	N.D.	N.D.	
	Febuxostat 90 mg/kg	N.D.	N.D.	

N.D., Under detection limit (< 2.42 ng/mL)
[a]Mean ± S.D. (N=4)
*p < 0.05; **p <0.01, significantly different from the vehicle group

Supplementary Table 3

Effect of lapatinib on biliary excretion of daidzein and its conjugate metabolites after oral administration of daidzein in mice[a]

Compounds	Treatment	0-1 h[b] (ng)	1-2 h[b] (ng)	2-3 h[b] (ng)	3-4 h[b] (ng)
Daidzein	Vehicle	$1.86\times10\pm0.65\times10$	$6.44\times10\pm3.89\times10$	$1.66\times10^2\pm0.99\times10^2$	$6.46\times10\pm3.08\times10$
	Lapatinib	$1.25\times10\pm0.82\times10$	$3.91\times10\pm1.09\times10$	$2.53\times10^2\pm1.72\times10^2$	$4.69\times10\pm4.16\times10$
DS	Vehicle	$8.66\times10^2\pm3.46\times10^2$	$2.19\times10^3\pm1.06\times10^3$	$7.70\times10^2\pm4.39\times10^2$	$8.35\times10^2\pm2.34\times10^2$
	Lapatinib	$4.41\times10^2\pm0.95\times10^2$	$1.18\times10^3\pm0.53\times10^3$	$2.88\times10^2\pm0.34\times10^2$	$3.85\times10^2\pm1.22\times10^2$*
DG	Vehicle	$0.92\times10^2\pm0.73\times10^2$	$3.98\times10^2\pm2.34\times10^2$	$5.13\times10^2\pm3.10\times10^2$	$1.72\times10^2\pm0.28\times10^2$
	Lapatinib	$0.96\times10^2\pm0.52\times10^2$	$3.58\times10^2\pm1.24\times10^2$	$5.91\times10^2\pm1.31\times10^2$	$1.90\times10^2\pm0.76\times10^2$

[a]Daidzein (3 mg/kg) was orally administered 1 h after oral administration of lapatinib (90 mg/kg) or vehicle alone.
[b]Bile was collected every 1 h following the lapatinib administration, and the amount of daidzein, DS, and DG were shown as mean ± S.D. (N=4)
*$p < 0.05$, significantly different from the control group.

Supplementary Table 4

Effect of lapatinib on urinary excretion of daidzein and its conjugate metabolites after oral administration of daidzein in mice[a]

Compounds	Treatment	blank[b] (ng)	0 -24 h[c] (ng)	24-48 h[c] (ng)
Daidzein	Vehicle	$2.94x10^3 \pm 0.63x10^3$	$9.59x10^3 \pm 0.75x10^3$	$1.42x10^4 \pm 0.52x10^4$
	Lapatinib	$2.87x10^3 \pm 0.18x10^3$	$1.01x10^4 \pm 0.09x10^5$	$1.53x10^4 \pm 0.70x10^4$
DS	Vehicle	$1.14x10^5 \pm 0.27x10^5$	$1.34x10^5 \pm 0.84x10^5$	$1.77x10^5 \pm 0.62x10^5$
	Lapatinib	$1.62x10^5 \pm 0.29x10^5$	$1.55x10^5 \pm 0.59x10^5$	$2.13x10^5 \pm 0.59x10^5$
DG	Vehicle	$1.24x10^4 \pm 0.27x10^4$	$2.10x10^4 \pm 1.38x10^4$	$4.22x10^4 \pm 1.50x10^4$
	Lapatinib	$1.22x10^4 \pm 0.17x10^4$	$2.80x10^4 \pm 1.38x10^4$	$4.12x10^4 \pm 0.81x10^4$

[a]Daidzein (3 mg/kg) was orally administered 1 h after oral administration of lapatinib (90 mg/kg) or vehicle alone.

[b]Blank urine sample was collected for 24 h before lapatinib administration, and the amount of daidzein, DS, and DG were shown as mean ± S.D. (N=3-4)

[c]Urine was collected every 24 h after daidzein administration, and the amount of daidzein, DS, and DG were shown as mean ± S.D. (N=3-4)

Supplementary Figure 1

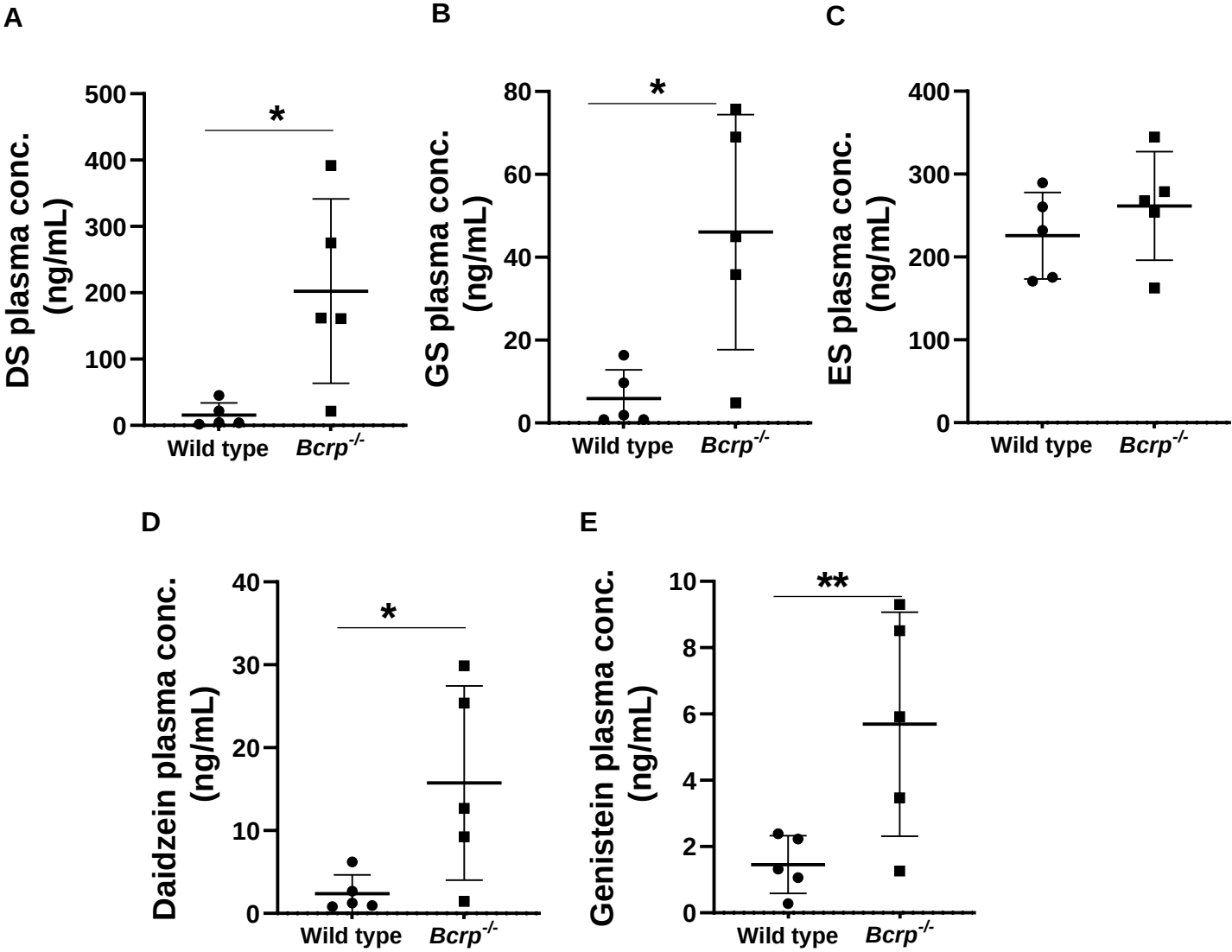

Supplementary Figure 1
Plasma concentration of isoflavone sulfates and their parent compounds in wild-type (●) and *Bcrp*$^{-/-}$ (■) mice under normal food ingestion. Plasma concentration was measured using LC-MS/MS, and data are expressed as mean ± S.D. (N = 5). Equol was under detection limit (< 2.42 ng/mL).
*$p < 0.05$, **$p < 0.01$, significantly difference from wild-type mice.

Supplementary Figure 2

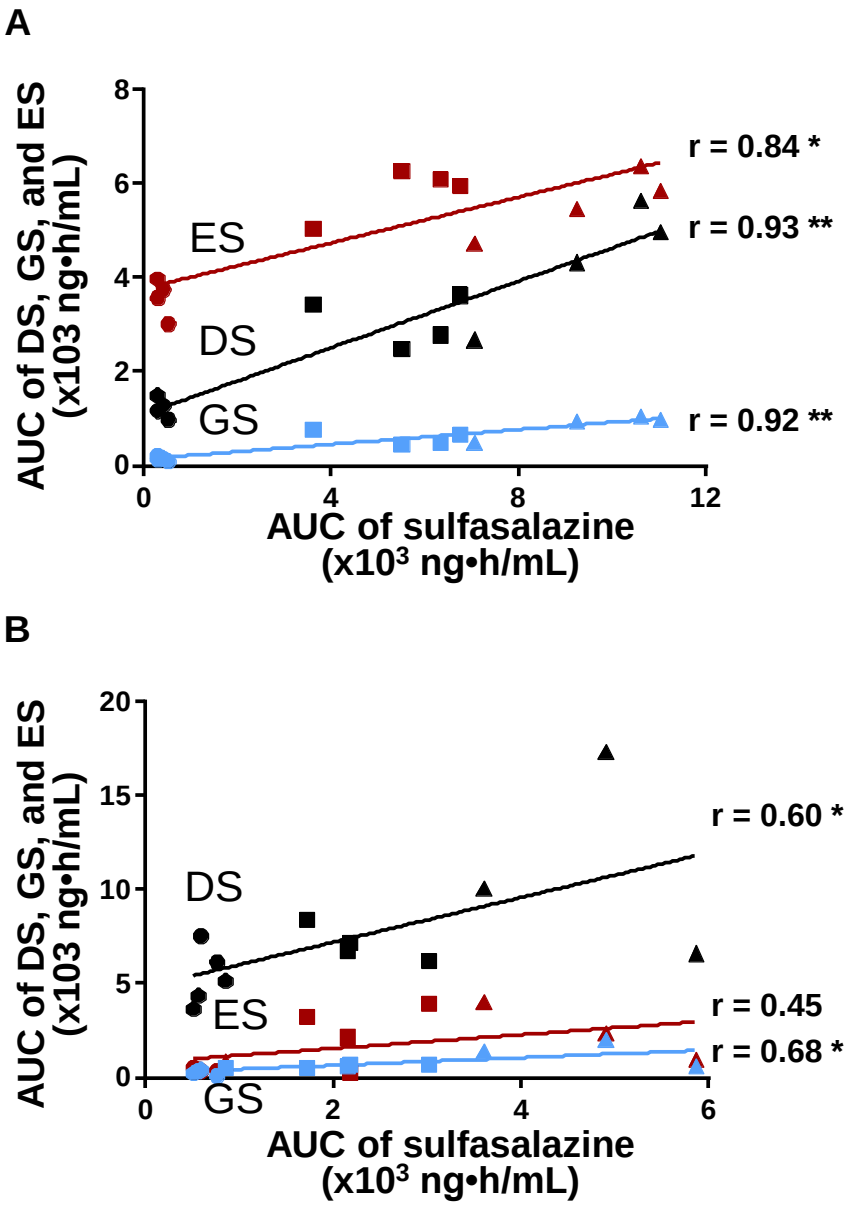

Supplementary Figure 2
Correlation between AUC of sulfasalazine and that of DS, GS, and ES.
AUC of sulfasalazine, DS, GS, and ES were obtained in each mouse after oral administration of vehicle alone, and lapatinib (30 and 90 mg/kg, A) or febuxostat (30 and 90 mg/kg, B). Individual data were plotted, and correlation analysis was performed in GraphPad software. **p < 0.01, *p < 0.05, significant correlation was observed (Pearson r analysis).

Supplementary Figure 3

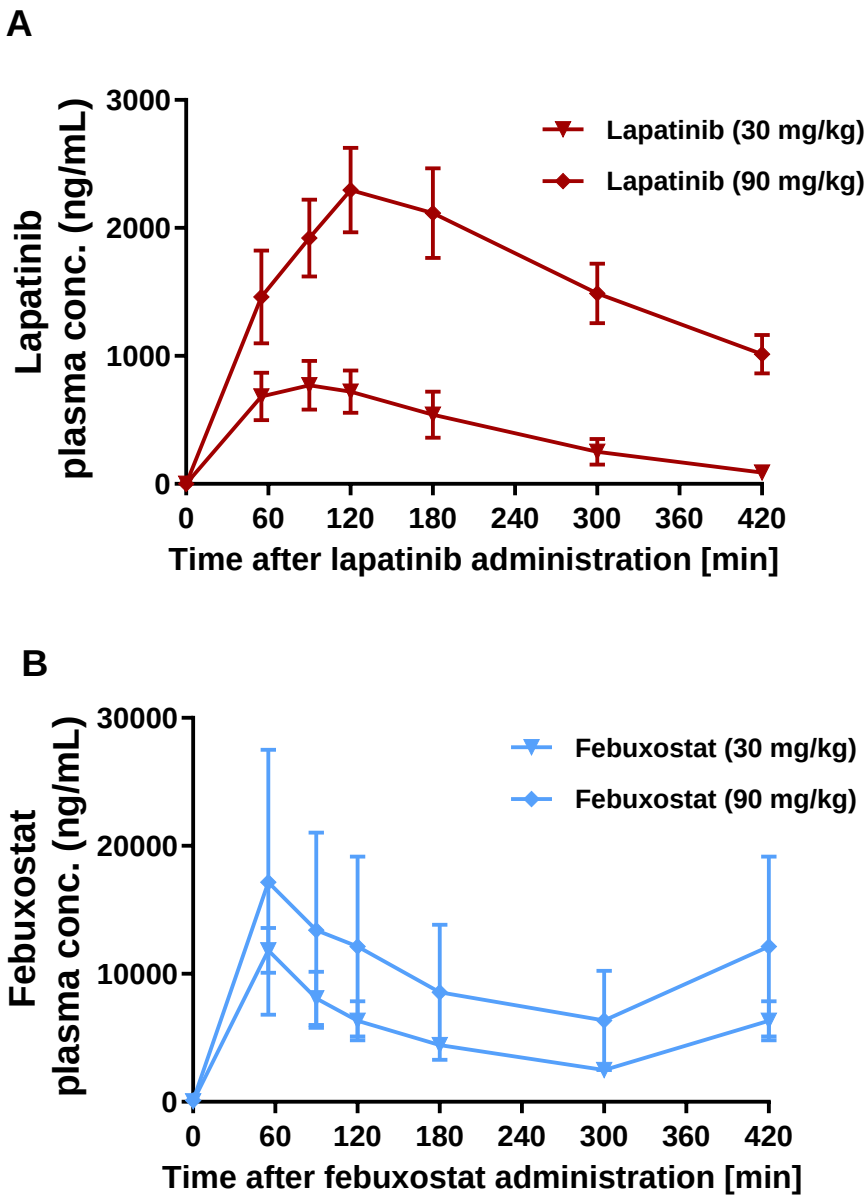

Supplementary Figure 3
Plasma concentration profiles of lapatinib and febuxostat in mice. Plasma concentration was measured using LC-MS/MS, and data were expressed as mean ± S.D. (N = 4).

Supplementary Figure 4

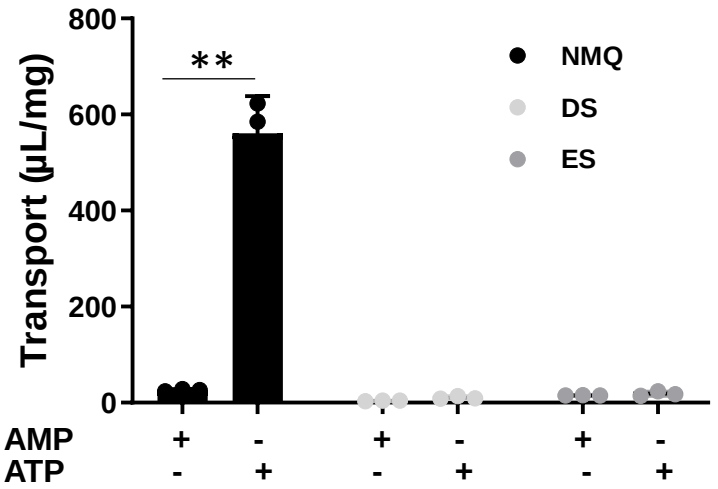

Supplementary Figure 4

Transport of DS and ES by P-gp expressing membrane vesicle. The uptake of NMQ, DS and ES by the membrane vesicles was measured in the presence of ATP or AMP. Data were expressed as mean ± S.D. (N = 3). **p < 0.01, significantly difference from AMP group.

Supplementary Figure 5

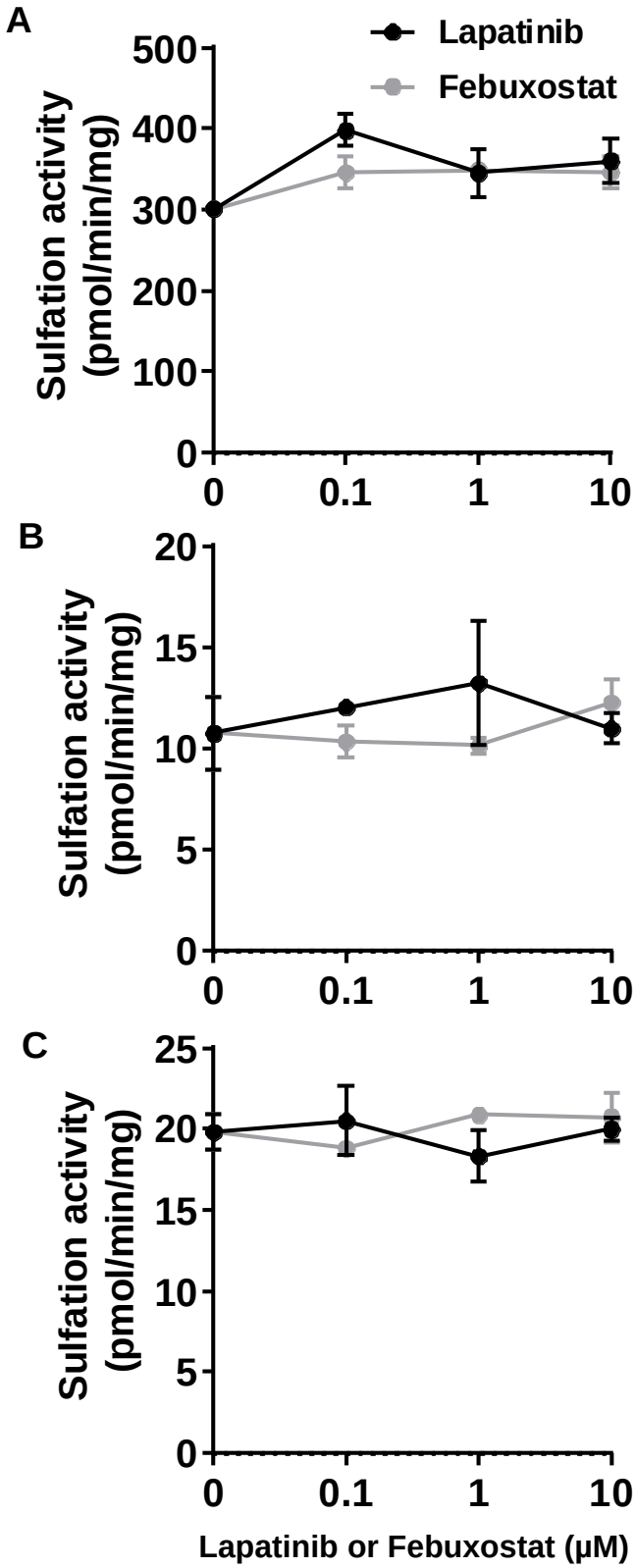

Supplementary Figure 5

BCRP inhibitors do not affect sulfate conjugation of isoflavones in cytosols prepared from mouse small intestines. Daidzein (A), genistein (B), and equol (C) (20 μM for each) were individually incubated with cytosols prepared from mouse small intestines. Incubations was performed in the presence of lapatinib and febuxostat (0, 0.1, 1, and 10 μM). Concentrations of DS, GS, and ES in the reaction mixture were measured by LC-MS/MS, and formation rate was normalized by protein amount and reaction time. Each value represents the mean ± S.D. (N =3).